PLANT SCIENCES



# DOG1 controls dormancy independently of ABA core signaling kinases regulation by preventing AFP dephosphorylation through AHG1

**Thorben Krüger[1], Dennis Brandt[1], Johanna Sodenkamp[1], Michael Gasper[1], Maida Romera-Branchat[1], Florian Ahloumessou[1,2]†, Elena Gehring[1], Julia Drotleff[1], Christopher Bell[1]‡, Katharina Kramer[3], Jürgen Eirich[1], Wim J. J. Soppe[4,5], Iris Finkemeier[1,3], Guillaume Née[1,4]***

**Seed dormancy determines germination timing, influencing seed plant adaptation and overall fitness. DELAY OF GERMINATION 1 (DOG1) is a conserved central regulator of dormancy cooperating with the phytohormone abscisic acid (ABA) through negative regulation of ABA HYPERSENSITIVE GERMINATION (AHG) 1 and AHG3 phosphatases. The current molecular mechanism of DOG1 signaling proposes it regulates the activation of central ABA-related SnRK2 kinases. Here, we unveil DOG1's functional autonomy from the regulation of ABA core signaling components and unravel its pivotal control over the activation of ABSCISIC ACID INSENSITIVE FIVE BINDING PROTEINs (AFPs). Our data revealed a molecular relay in which AFPs' genuine activation by AHG1 is contained by DOG1 to prevent the breakdown of maturation-imposed ABA responses independently of ABA-related kinase activation status. This work offers a molecular understanding of how plants fine-tune germination timing, while preserving seed responsiveness to adverse environmental cues, and thus represents a milestone in the realm of conservation and breeding programs.**

## INTRODUCTION

With its remarkable resilience features, the seed represents a pivotal evolutionary innovation of plants fostering colonization of terrestrial areas (*1*, *2*). The commitment to germination signifies the conclusion of the resilience phase; thus, precise control of this process is paramount for success. Unfavorable environmental conditions during seed imbibition prevent germination (*3*). In addition, dormancy sensu stricto, an evolutionary and adaptative trait, restrains the sprouting of viable seeds, even under optimal conditions (*4*). Primary dormancy is established during seed maturation and is gradually released during dry storage (so-called after-ripening) or by environmental stimuli at imbibition (*5*). It ensures seedling establishment in the proper season, soil seed bank maintenance, promotes dispersal, and contributes to germination betting strategies (*6*).

The plant hormone abscisic acid (ABA), acting as a general growth inhibitor, is involved in many plant developmental processes and stress responses (*7*). Plants defective in ABA synthesis, perception, or core signaling transduction processes produce nondormant seeds that cannot restrict their germination under stressful conditions (*8*–*11*). Degradation of ABA during imbibition promotes sprouting, while its de novo synthesis is required to prevent germination under stress or in dormant seeds (*12*–*16*). Hence, ABA is essential for primary seed dormancy induction during maturation as well as during imbibition to inhibit germination of dormant or nondormant seeds under optimal or stress conditions, respectively. Dormancy loss slightly enlarges the environmental window permitting germination, but seeds' stress reactiveness is largely preserved, indicating this trait to be distinct from stress responses (*17*). Dormancy alleviation mechanisms occurring in dry seeds are elusive but recognized to interact with the ABA-dependent germination arrest program upon imbibition (*18*). While both traits are undoubtedly dependent on ABA, the molecular framework by which seeds accommodate dormancy release while maintaining their capacity to stop germination if cues are met is not yet understood. Genetic determinants involved in the dormancy alleviation mechanisms during dry storage were identified by studying *Arabidopsis* natural variation in the length of after-ripening time required for germination (*19*). The gene underlying the major quantitative trait loci effect, *DELAY OF GERMINATION 1* (*DOG1*), was shown to be required for seed dormancy and central for the local adaption of this trait to environmental conditions (*20*–*25*). Although DOG1 and ABA are both required for dormancy, these master regulators do not operate in a linear genetic pathway (*13*, *25*).

ABA core signaling pathway consists of REGULATORY COMPONENT OF ABA RECEPTORs (RCARs), which bind ABA and consequently inhibit clade A PP2C phosphatases (PP2CAs) to prevent inhibitory dephosphorylation of class III SNF1-RELATED PROTEIN KINASEs of group 2 (SnRK2IIIs). Phosphorylation of SnRK2III substrates downstream of the ABA core signaling leads to the activation of physiological ABA responses (*7*). *DOG1* encodes a protein of unknown molecular function (*25*). We previously found that DOG1 controls dormancy by physically interacting with ABA HYPERSENSITIVE GERMINATION 1 (AHG1) and AHG3 to negatively regulate their functions in vivo (*26*). AHG1, an atypical PP2CA, is an exceptional feature of the seed ABA signalosome and refractory to RCAR inhibition but negatively regulates ABA responses in vivo, like most PP2CAs (*27*, *28*). Its genuine control by

[1]Institute of Plant Biology and Biotechnology, University of Münster, Münster, 48149, Germany. [2]West Africa Centre for Crop Improvement, University of Ghana, Legon, Ghana. [3]Plant Proteomics, Max Planck Institute for Plant Breeding Research, Cologne, 50829, Germany. [4]Department of Plant Breeding and Genetics, Max Planck Institute for Plant Breeding Research, Cologne, 50829, Germany. [5]Rijk Zwaan, De Lier, 2678 ZG, Netherlands.
*Corresponding author. Email: neeg@uni-muenster.de
†Deceased.
‡Present address: Department of Biology, University of Oxford, Oxford, OX1 3RB, UK.

DOG1 explains the requirement of both DOG1 and ABA for dormancy (*26*). An independent report confirmed the existence of the DOG1-PP2C module and further proposed a direct inhibition of AHG1's catalytic activity by DOG1 to maintain SnRK2IIIs phosphorylated, thereby active (*29*). SnRK2III regulation by DOG1 would imply dormancy alleviation to be linked with desensitization to adverse conditions, thus disabling competitive advantages conferred by the seed habit. Noteworthy, null mutations of *DOG1* abolish dormancy but have minor effects on the seed sensitivity to ABA (*25*, *26*). Hence, the DOG1-ABA molecular intertwining in the control of dormancy remains unresolved.

Using a proteomic-genetic integrated approach, we demonstrate that the DOG1-PP2C module does not participate in the control of SnRK2III activity in vivo and, thus, that DOG1 controls dormancy independently of the ABA core signalosome activation. We identified a conserved phosphorylation site in two ABSCISIC ACID INSENSITIVE FIVE BINDING PROTEINs (AFPs) decreased in abundance in *dog1-1* mutant seeds. We reveal that AHG1 physically interacts with AFPs and is essential for their role in regulating seed dormancy. Furthermore, our data demonstrate that AFPs are indispensable for the functionality of the DOG1-PP2C module in controlling seed dormancy, highlighting their critical role in this regulatory pathway. Last, through the combination of mutant alleles at different steps of the proposed pathway, we present a compelling case validating, in planta, a DOG1 signaling pathway that operates alongside the SnRK2III hub of the ABA core signaling to regulate ABA responses and oversees the dormancy trait. Our findings elucidate, at the molecular level, how seeds adjust the timing of germination with minimal impact on their capacity to prevent sprouting under unfavorable conditions.

## RESULTS

### DOG1 shapes the dry and early imbibed seed proteome and phosphoproteome

The prevailing molecular model for DOG1's mode of action proposes that it prevents SnRK2III deactivation by repressing specific clade A PP2Cs, notably AHG1, thereby maintaining the ABA responses required to inhibit germination. Consequently, the relief of AHG1 negative regulation in *dog1* null mutants is expected to trigger SnRK2III repression during imbibition. To further investigate this hypothesis, we used the *abi2-1* mutant as a well-characterized genetic background for PP2CA inhibition relief. The G to D mutation in *abi1-1* or *abi2-1* prevents these PP2CAs from interacting with ABA receptors, leading to the constitutive repression of SnRK2III activity (*30*). We directly compared the dormancy and stress responsiveness of *dog1-1* and *abi2-1* seeds and found that both mutants are fully nondormant at harvest (fig. S1A). However, in the presence of ABA, *dog1-1* seeds largely retain their ability to inhibit germination, whereas *abi2-1* seeds completely lose this capacity (fig. S1, B and C). These findings demonstrate that SnRK2III responses remain functional in the *dog1-1* mutant, suggesting that its regulation is unlikely to be the primary mechanism by which the DOG1-PP2C module controls seed dormancy.

To identify relevant downstream targets controlled by the DOG1-PP2C module in vivo, we performed a quantitative mass spectrometry analysis comparing the proteome and phosphoproteome of freshly harvested dormant NIL-DOG1 with nondormant *dog1-1* seeds in dry and 6-hour imbibed seeds (Fig. 1, A and B, and table S1). The *dog1-1* mutation affects 10.8% (dry) and 13.1% (imbibed) of the quantified protein groups and induced alterations in the seed phosphoproteome, with 19.9% (dry) and 8.6% (imbibed) of the quantified phosphopeptides (p-peptides) being significantly changed in abundance in mutant compared to NIL-DOG1 seeds (Fig. 1, C to F). Coherently with the predisposition of *dog1-1* seeds to germinate at harvest, up-regulated proteins were enriched in active metabolism, while down-regulated proteins were enriched in stress and seed dormancy-associated Gene Ontology (GO) terms (Fig. 1G). Proteins with regulated p-peptides were enriched in the GO terms cytosol and nucleus, as well as in RNA splicing, and ABA responses (Fig. 1H). This aligns with DOG1's role in regulating the function of AHG1 and AHG3.

### DOG1 stabilizes ABA responses during maturation and imbibition

To investigate the status of ABA responses in *dog1-1* seeds, we mined our proteomic data and found in either or both dry and imbibed seeds significantly regulated proteins annotated with the GO term "response to ABA." This included well-known markers for positive ABA responses such as EM1, EM6, and RD29B that we found down-regulated in *dog1-1* compared to NIL-DOG1 (fig. S2, A and B). We further compared significant regulation between genotypes for all ABA-responsive proteins with changes observed at the mRNA levels in mutants defective in ABA synthesis and catabolism (*31*). Although our data likely reflect only a part of the ABA responses in seeds, we found that the regulations of ABA-responsive proteins in *dog1-1* are opposite to the effect of endogenous ABA (fig. S2, C and D). When further analyzing ABI5 protein levels, we observed a significantly impaired accumulation in *dog1-1* compared to NIL-DOG1 dry and imbibed seeds (fig. S2, E and F). Hence, our data show that during the end of maturation and early imbibition of freshly harvested seeds, DOG1 is required to properly establish ABA responses at the proteome level.

### DOG1 functions independently of SnRK2III activation and SnRK2.6 activity in vivo

P-peptides from 14 proteins implied in ABA responses, including 9 (cyto-)nuclear phosphoproteins, were significantly changed in abundance between genotypes in dry or imbibed seeds (table S2). As a hallmark, we found a p-peptide from SnRK2III activation loop to be more abundant in *dog1-1* compared to NIL-DOG dry seeds (Fig. 2, A to C). This peptide is modified at a position (i.e., S171 in SnRK2.6) directly associated with SnRK2III ABA-dependent upstream activation (*32*–*35*). The detected phosphopeptide in dry seed tissue is shared between all SnRK2IIIs; hence, it can originate from any isoforms. We therefore examined SnRK2III accumulation in dry seeds using an antibody recognizing all the three SnRK2IIIs. We found protein levels to be similar in both genotypes (Fig. 2D). The normalization of p-peptide regulation on protein abundance indicated the activation mark residue of SnRK2IIIs to be approximately four times more phosphorylated in *dog1-1* compared to NIL-DOG1 (Fig. 2E). To further address the effect of DOG1 on ABA core signaling kinase, we tested the impact of its loss of function on the activation and activity of SnRK2.6, which was used as representative example for SnRK2IIIs. We generated transgenic lines expressing a yellow fluorescent protein (YFP):SnRK2.6 fusion protein in both NIL-DOG1 and *dog1-1* backgrounds (fig. S3, A and B). The fusion construct localized in the nucleus and cytosol of 6- and 24-hour

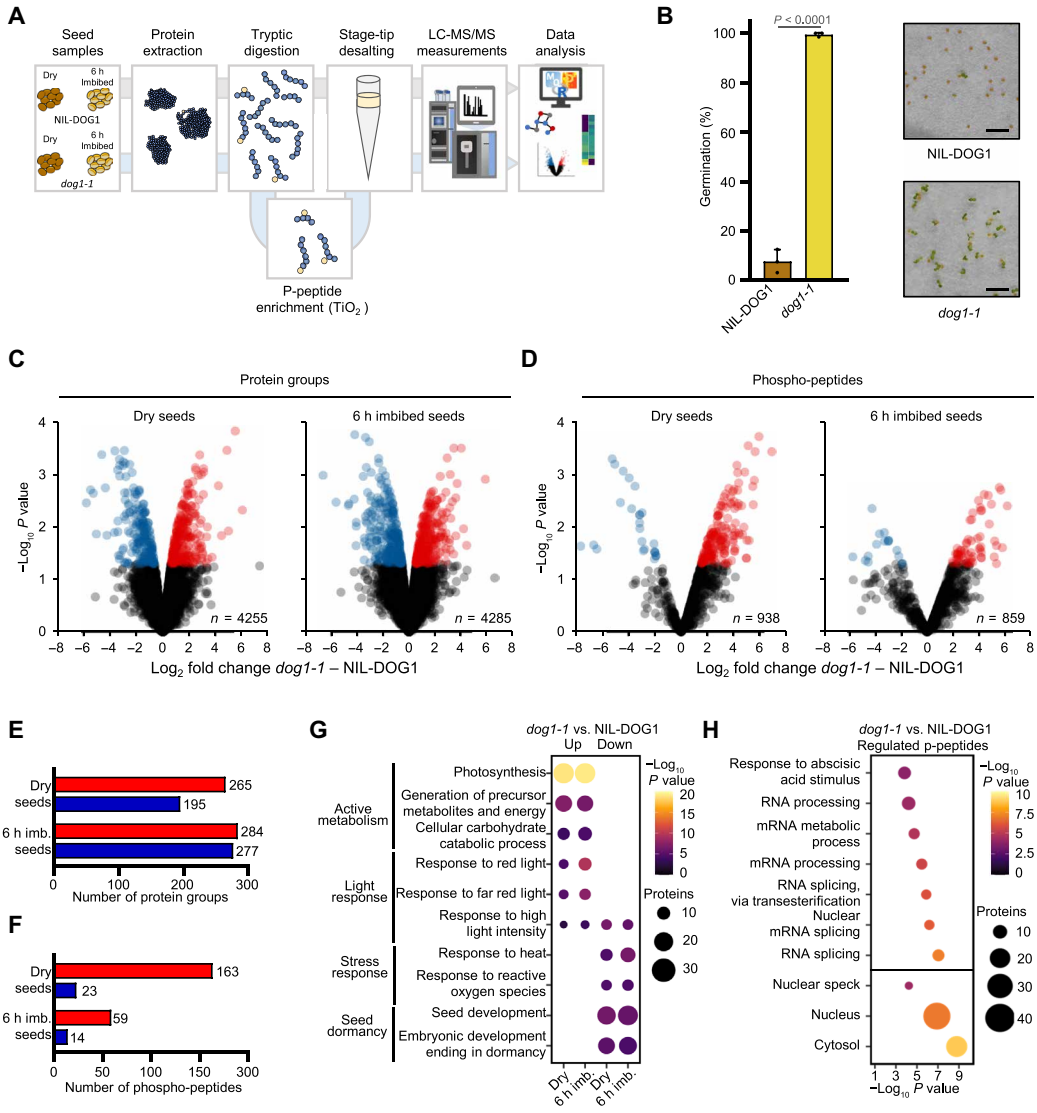


**Fig. 1. Proteome and phosphoproteome analyses of freshly harvested NIL-DOG1 and *dog1-1* seeds in the dry and 6-hour water imbibed state.** (**A**) Schematic workflow of the proteome analysis. Peptides for proteome and phosphoproteome analyses were prepared from the same seed extract and analyzed in parallel. (**B**) Germination capacity of NIL-DOG1 and *dog1-1* seeds at the sampling time of the proteomic experiments (means ± SD, $n = 3$ biological replicates, unpaired $t$ test $P$ value is indicated). Scale bars, 2 mm. (**C** and **D**) Volcano plots showing the regulation of (C) protein group abundance or (D) phosphopeptide abundance in dry (left) and 6-hour imbibed (right panel) seeds of *dog1-1* compared to NIL-DOG1. (**E**) Number of protein groups and (**F**) p-peptides with significant changes ($P$ value < 0.05) in abundance between genotypes. In (C) to (F), down- and up-regulation are shown in blue and red, respectively. (**G**) GO enrichment for biological processes in dry or imbibed (imb.) seeds of proteins significantly regulated between genotypes. (**H**) GO biological process (top) and cellular component enrichment (bottom) of all (up- and down-regulated) phosphoproteins with significantly regulated p-peptide abundances either in dry, imbibed, or in both conditions. h, hours.

imbibed seeds embryos independently of the genetic background (fig. S3C). We used targeted proteomics to examine the modification status by phosphorylation of both S171 and S175/T176 after immunoprecipitation of the fusion protein from dry seed extracts of both backgrounds (fig. S4, A and B). We found these residues to be more phosphorylated in *dog1-1* compared to NIL-DOG1 (fig. S4, C to E). Next, we compared the kinase activity of YFP:SnRK2.6 purified from dry seeds of the two backgrounds and found that the kinase was more than two times more active when extracted from *dog1-1* compared to NIL-DOG1 seeds, aligning with their respective activation status (Fig. 2F). Together, our data directly demonstrate that in vivo DOG1's function is not to prevent the deactivation of SnRK2IIIs as loss of *DOG1* function rather promotes their activation by phosphorylation at a conserved residue which leads to increased SnRK2.6 activity in seeds.

Two p-peptides from group A bZIP C1 and C2 domains were found to be more abundant in *dog1-1* compared to NIL-DOG1 seeds (fig. S5). This aligns with a higher SnRK2III activity in mutant seeds (*36*). Efficient SnRK2III inhibition involves dephosphorylation of their activation loops and insertion into their catalytic clefts of a tryptophan conserved in PP2CAs and so-called Trp-lock (*37*). This residue is not conserved in AHG1 and its monocotyledon

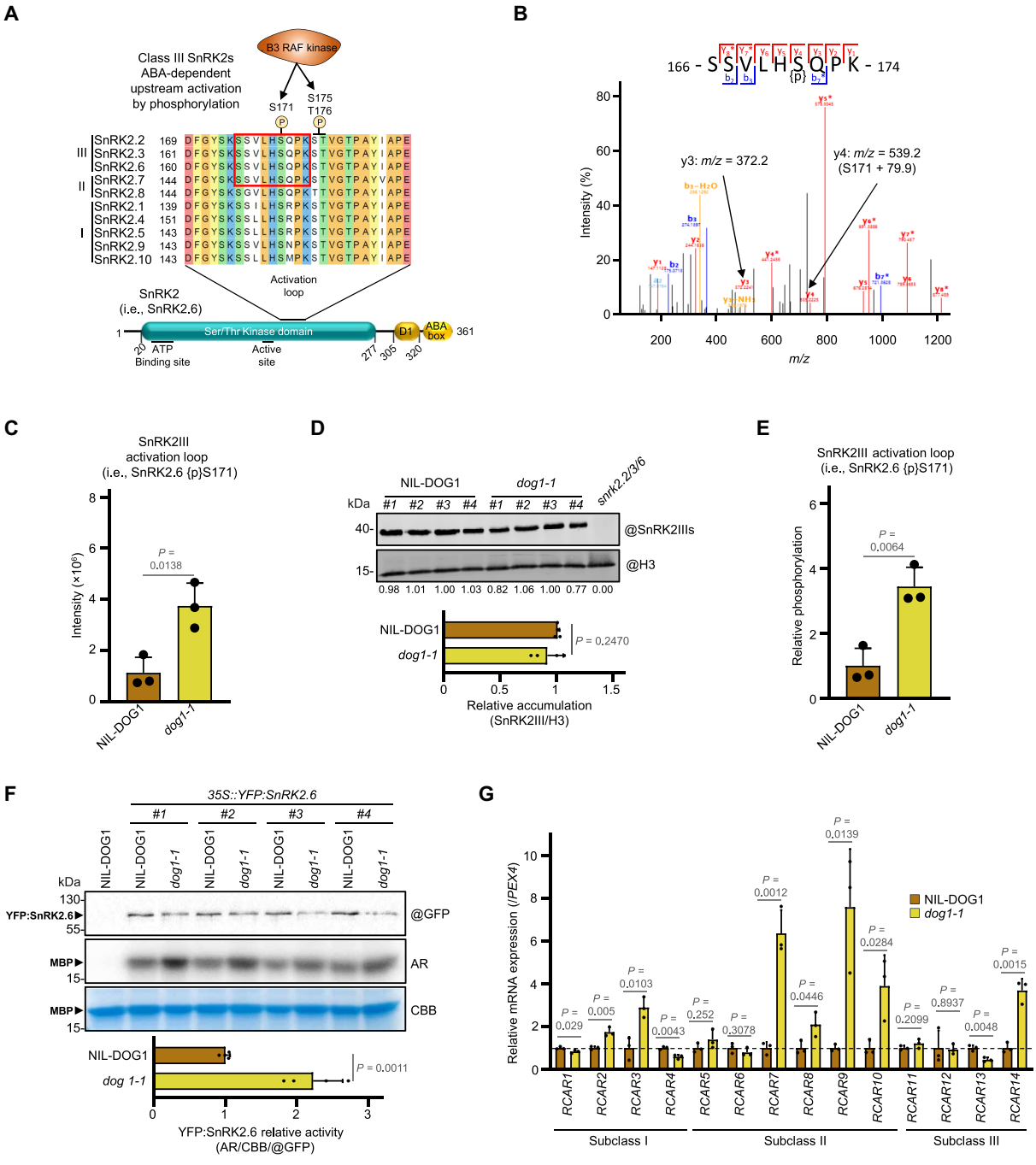


**Fig. 2. ABA core signaling is primed in *dog1-1* seeds.** (**A**) Schematic representation of SnRK2III protein (using SnRK2.6 as an example) and of amino acid sequence alignment of *Arabidopsis* SnRK2s' activation loops. The tryptic p-peptide more abundant in *dog1-1* compared to NIL-DOG1 is highlighted in red. Phosphorylation of SnRK2III activation loop is mediated by RAF kinases. (**B**) $MS^2$ spectrum of the tryptic peptide phosphorylated at S171 (in SnRK2.6). *m/z*, mass/charge ratio. (**C**) $MS^1$ intensities of the SnRK2III activation loop p-peptide in dry NIL-DOG1 and *dog1-1* seeds (means ± SD, $n = 3$ biological replicates). (**D**) Western blot quantification of SnRK2IIIs in dry NIL-DOG1 and *dog1-1* seeds. The bar chart shows protein SnRK2III accumulation normalized to the histone 3 (H3) loading control (means ± SD, $n = 4$ biological replicates). (**E**) Phosphorylation of SnRK2III activation loop between dry NIL-DOG1 and *dog1-1* seeds after normalization of peptide intensity to the protein abundance change (means ± SD, $n = 3$ biological replicates). (**F**) Kinase activity of YFP-SnRK2.6 immunoprecipitated from dry seed of NIL-DOG1 and *dog1-1* background. YFP-SnR2.6–bound beads were used to phosphorylate MBP in vitro in the presence of $^{32}P$ γ-ATP. The phosphorylation of MBP with radiolabeled phosphate was assessed using autoradiography (AR), loading of MBP was evaluated by Coomassie Brilliant Blue (CBB) staining, and the amount of YFP:SnRK2.6 was investigated with anti-GFP. Signal intensities of phosphorylated MBP (autoradiography), total MBP (CBB), and YFP-SnRK2.6 (@GFP) amounts (bands marked with arrows) were determined by densitometric analyses. The bar chart shows the normalized (AR/CBB/@GFP) kinase activity (means ± SD, $n = 4$ biological replicates). IP from nontransgenic NIL-DOG1 protein extract served as the negative control. (**G**) Expression of the 14 *Arabidopsis* ABA receptors from the *RCAR* family in dry seeds of NIL-DOG1(means ± SD, $n = 3$ biological replicates). The data presented in (C) to (G) show levels relative to NIL-DOG1 (arbitrary mean value of 1), and unpaired *t* test *P* values are indicated. In (D) and (F), "#" indicates independent biological replicates.

orthologs (fig. S6, A and B). Molecular modeling suggests AHG1 to be unable to occupy SnRKIII active site compared to canonical PP2CAs (fig. S6C). To address whether the enhanced SnRK2III activation in *dog1-1* was associated with an increased sensitization to ABA, we analyzed transcript levels of the 14 *Arabidopsis* ABA receptors in dry NIL-DOG1 and *dog1-1* seeds (Fig. 2G). We found that the expression of seven *RCARs* was significantly up-regulated in *dog1-1* (up to seven times), while three receptors were down-regulated (maximum twofold). Together, our results indicate that the ABA core signaling pathway activity is primed in *dog1-1* seeds. Yet, this activation does not override the nondormant phenotype of *dog1-1* seeds. Consequently, the DOG1-PP2C module must operate via a molecular mechanism distinct from the regulation of SnRK2III activation.

### The redundant negative regulators of seed dormancy, AFP1 and AFP2, are less phosphorylated in *dog1-1*

Since DOG1 negatively regulates AHG1 and AHG3 phosphatases in the nucleus, we searched for nuclear proteins that were less phosphorylated in *dog1-1* mutants. Our analysis identified p-peptides deriving from AFP1 and AFP2 modified at S115 and S112, respectively (fig. S7, A and B). This residue is conserved in all four *Arabidopsis* AFPs and located in their B-domain (fig. S7C). The AFP1 p-peptide was found to be eight times less abundant in dry seeds of *dog1-1* compared to NIL-DOG1 (Fig. 3A). Protein quantification revealed AFP1 abundance to be reduced by 50% in *dog1-1* dry seed (Fig. 3B). The normalization of the p-peptide change relative to the protein change revealed that the AFP1 protein pool was about four times less phosphorylated at S115 compared to NIL-DOG1 (Fig. 3C). Our data also indicated that the AFP2 p-peptide was less abundant in imbibed mutant seeds compared to NIL-DOG1 (table S2). Similar to *DOG1* and *AHG1*, the expression of *AFPs* is mainly restricted to seed tissues (fig. S8A). As the maternal environment strongly influences primary seed dormancy levels in *Arabidopsis* (*18*), we examined whether *AFP* expression is responsive to temperature stimuli during seed maturation, resulting in contrasting dormancy at harvest (fig. S8, B and C). The expression of all four *AFPs* was significantly lower in dormant compared to nondormant seed batches (fig. S8D), indicating an association between dormancy levels and *AFP* expression. To address the importance of the different AFPs in the control of seed dormancy sensu stricto, we characterized this trait for single and multiple *afp* mutants. Our analysis demonstrated that AFP1, AFP2, and AFP3 act as partially redundant negative regulators of dormancy (fig. S9A). The hyperdormant phenotype of the triple *afp1-5/2-2/3-1* mutant was still observable in seed batches obtained from conditions resulting in shallow dormancy of Col-0 seeds at harvest (fig. S9B). We did not observe an enhancement of the *afp2-2* phenotype by the *afp4-2* mutant allele (fig. S9C). Potent ectopic overexpression of *AFPs* leads to severe maturation defects and compromises the viability of homozygous *35S::YFP:AFP2* seeds (*38*, *39*) . Thus, we analyzed the dormancy of seed progenies from *35S::YFP:AFP2* (+/−) hemizygous parental lines. Despite being produced in a dormancy-promoting maternal environment, we found that transgenic seeds were fully nondormant compared to Col-0 (fig. S10, A and B), confirming that AFPs are negative regulators of seed dormancy. To further address the importance of ABA level dynamics for AFPs to control germination, we used fluridone or abscinazole-E3M (ABZ-E3M) to prevent ABA de novo synthesis or catabolism, respectively. While fluridone effectively promoted the germination of freshly harvested Col-0 seeds, the *afp1-5/2-2/3-1* triple mutant seeds were not responsive to this treatment (fig. S9D). ABZ-E3M significantly reduced germination of after-ripened Col-0 but not *35S::YFP:AFP2* (+/−) seed progenies (fig. S10C). Thus, the function of AFP in the control of germination appears independent of ABA metabolism during imbibition. These findings prompted us to investigate the involvement of AFPs in the regulation of seed dormancy by the DOG1-PP2C module.

### AFPs specifically interact with AHG1 in vivo

To investigate whether the regulation of AFP phosphorylation observed in the *dog1-1* mutant results from the relief of DOG1-mediated negative regulation on some PP2CAs, we first examined in vivo the physical protein interactions between the four AFPs and the nine PP2CAs of *Arabidopsis* in a yeast two-hybrid system. We observed that all AFPs exclusively interacted with AHG1 (Fig. 3D and fig. S11). We then confirmed the specificity of the AFP-AHG1 interactions in planta by conducting coimmunoprecipitation (co-IP) assays using *Nicotiana benthamiana* leaves transiently coexpressing *Venus:AFPs* and *3xHA:PP2CAs* (fig. S12). Next, we questioned whether the amino acid sequence context around the B-domain phosphorylation sites of AFP1 and AFP2 could limit AHG1's ability to directly use AFPs as substrates. We used a recombinant AHG1 protein with verified quality and activity to assess its in vitro capacity to dephosphorylate the aforementioned AFP1 and AFP2 phosphoserines ({pS}) using 13–amino acid–long synthetic phosphopeptides (fig. S13, A to C). Our results showed that AHG1 effectively dephosphorylates AFP1{pS}115 and AFP2{pS}112 phosphopeptides (Fig. 3E). In contrast, AHG1 displayed no activity toward a phosphopeptide containing the sequence context of the SnRK2III phosphoserine, which is hyperphosphorylated in the *dog1-1* mutant (Fig. 3E and fig. S12D). Together, our in vivo interaction and in vitro assay data suggest that the phosphosite in the B-domain of AFPs may serve as a substrate for AHG1.

### AFP2 requires AHG1 to control germination

To investigate the requirement of AHG1 for AFP2 functions in vivo, we crossed the *AFP2* overexpression line with *ahg* mutants and isolated hemizygous *35S::YFP:AFP2* (+/−) plants in homozygous *ahg1-5* and *ahg3-2* backgrounds. While *YFP:AFP2* overexpression abolished dormancy in Col-0, we observed that seed progenies from *35S::YFP:AFP2* (+/−) in *ahg1-5* germinated to a lower extent compared to Col-0 seeds (Fig. 3F). These data demonstrate that AHG1 is genetically required for AFP2 to function in the control of dormancy. The seed progenies from *35S::YFP:AFP2* (+/−) in the *ahg3-2* background exhibited only a marginal increase in dormancy compared to the seed batches from *35S::YFP:AFP2* (+/−) in the Col-0 background. This indicates that AFP2's function during germination is not dependent on AHG3, which is in line with the specific interactions of AFPs with AHG1.

### The nondormant phenotype of *dog1* seeds is partially dependent on AFP1 and AFP2

To investigate the genetic relationship between DOG1 and AFPs, we generated combinatorial *afp* and *dog1-2* mutants. Germination analysis of double to quadruple mutant seeds showed that, in contrast to *dog1-2*, the triple *afp1-5/2-2 dog1-2* mutant produces about 25% of dormant seeds. The additional mutation of *afp3-1* in the quadruple mutant did not further enhance the dormancy levels in the context

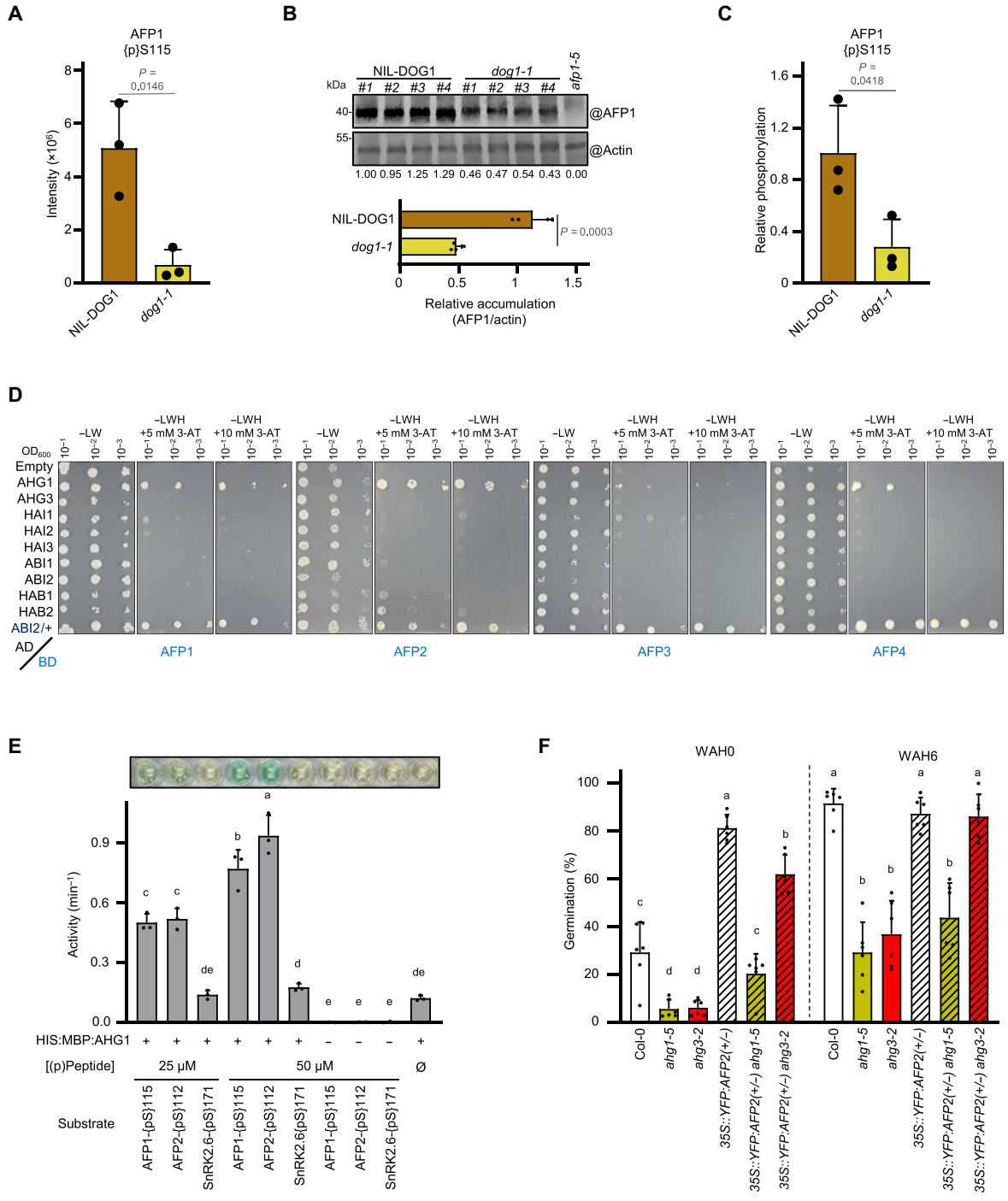


**Fig. 3. AFPs are substrates of AHG1, and AFP2 functionally requires AHG1 to control germination *in vivo*.** (**A**) MS intensity of AFP1 p-peptides containing {pS}115 (means ± SD, $n = 3$ biological replicates). (**B**) Western blot quantification of AFP1 in dry NIL-DOG1 and *dog1-1* seeds. The bar chart shows protein accumulation of AFP1 normalized to the actin loading control (means ± SD, $n = 4$ biological replicates). (**C**) Phosphorylation of AFP1 {pS}115 between dry NIL-DOG1 and *dog1-1* seeds after normalization of peptide intensity to protein abundance change (means ± SD, $n = 3$ biological replicates). (**D**) Family-wide yeast two-hybrid screen between *Arabidopsis* clade A PP2Cs and AFPs. Control medium lacking leucine and tryptophan, –LW; interaction medium additionally lacking histidine, –LWH; 3-AT, 3-aminotriazole. Interaction of ABI2 with SnRK2.6 (+) served as positive control. Negative control assays for BD-AFP self-activation are shown in fig. S10. (**E**) In vitro phosphatase assays using HIS:MBP:AHG1 and synthetic phosphorylated peptides of AFP1{pS}115, AFP2{pS}112, and SnRK2III activation loop (i.e., SnRK2.6{pS}171). Assays in which the substrate or the enzyme was omitted served as negative controls (means ± SD, $n = 3$ independent assays). The top shows a representative picture of the colorimetric assay result. A positive control for SnRK2.6{pS}171 dephosphorylation is presented in fig. S12. (**F**) Germination capacity of seed progenies from *35S::YFP:AFP2*(+/–) in Col-0, *ahg1-5*, or *ahg3-2* mutant backgrounds compared to their parental lines at harvest and after 6 weeks after harvest (WAH) (means ± SD, $n = 6$ biological replicates). The data presented in (A) to (C) show levels relative to NIL-DOG1 (arbitrary mean value of 1), and unpaired *t* test *P* values are indicated. In (B), "#" indicates independent biological replicates. In (E) and (F), letters on the top of the bars indicate significantly different groups using a one-way analysis of variance (ANOVA) with a Tukey post hoc test ($\alpha = 0.05$).

of the *dog1-2* background (Fig. 4A). No effect of the *afp4-2* allele was observed when comparing seed dormancy of double *afp2-2 dog1-2* and triple *afp2-2/4-2 dog1-2* mutants (fig. S14A). We reproduced our results using independent *afp* mutant alleles (fig. S14B). Hence, *afp1* and *afp2* are sufficient to reintroduce dormancy in *dog1-2*, indicating that DOG1 signaling requires both AFP1 and AFP2.

### AFPs function downstream of the AHG1 branch

Our previous work showed that DOG1 relies on both AHG1 and AHG3 functions in planta (*26*). Here, we have shown that AFPs interact specifically with AHG1 and that this atypical PP2CA is essential for the function of AFP2 in seed dormancy (Fig. 3, D and F, and fig. S12). Hence, the activation of AHG3 might be responsible for the approximately 75% of germination in the *afp1-5 2-2 dog1- 2* triple mutant seed batches. We tested this hypothesis by combining *ahg3-2* and *afp* mutants. We found seed dormancy of *afp2-2 ahg3-2*, *afp1-5/2-2 ahg3-2*, and *afp2-2/3-1 ahg3-2* to be highly enhanced compared to their relative parents with an *AHG3* wild-type (WT) allele (fig. S15). Next, we analyzed the ability of *ahg3-2* to enhance seed dormancy of multiple *afp dog1-2* seeds. We observed that dormancy of the quadruple *afp1-5/2-2 ahg3-2 dog1-2* mutant was much stronger than the triple *afp1-5 2-2 dog1-2* or double *ahg3-2 dog1-2* mutant seeds at harvest (Fig. 4, B and C). This shows that the AHG1 branch of the DOG1-PP2C module requires AFP1 and AFP2 to control seed dormancy. We noted that, like the *ahg1-5/3-2 dog1-2* mutant, the dormancy level of quadruple *afp1-5/2-2 ahg3-2 dog1-2* or quintuple *afp1-5/2-2/3-1 ahg3-2 dog1-2* mutant seeds stayed stable even after extended storage (Fig. 4, B and C). The insensitivity of these mutant genotypes to afterripening indicates that they are unable to operate the molecular switch that normally permits growth after dormancy alleviation.

## DISCUSSION

The role of ABA in inducing growth arrest during stress responses can be traced back to the earliest land plants, although prototypical components of the ABA core signaling pathway are already present in algae (*2*). ABA responses evolved to reach their maximum intricacy in seed plants where, for example, ABA core signaling is encoded by multigenic families and embedded in a complex regulatory network. Such evolutive sophistication enabled the ubiquitous ABA signal to precisely control diverse physiological responses based on multiple developmental and environmental inputs (*28*). Dormancy is one of these phenomena. It is built up during maturation, but the resulting inhibition of sprouting takes place upon imbibition, accounting for differences in the germination level of seeds that have after-ripened or not. Although requiring ABA during seed maturation, dormancy depth is not directly correlated with ABA levels in dry seeds but is positively associated with DOG1 accumulation (*12*, *13*). ABA and DOG1 signaling pathways cross-talk at the level of the PP2CAs in the control of seed dormancy (*26*, *29*).

Here, we addressed the question whether DOG1 acts through modification of the canonical ABA core pathway, which is a long-standing debate in the seed biology and ABA signaling fields (*18*, *28*, *40*, *41*). In agreement with previous transcriptome studies (*42*), we found that DOG1 is required for the proper establishment of ABA responses at the proteome level during seed maturation and early imbibition (Fig. 1 and fig. S2). However, our data demonstrate that DOG1 does not play a role in preserving SnRK2IIIs in an active state in vivo. The phosphorylation of conserved SnRK2III residues associated with their activation is enhanced in nondormant *dog1-1* when compared to dormant NIL-DOG1 dry seeds (Fig. 2, A to E, and fig. S3). In agreement with enhanced activation marks, extractible SnRK2.6 activity from dry seed material was higher in *dog1-1* compared to NIL-DOG1 (Fig. 2F), but we did not directly test the influence of DOG1 on the two other SnRK2IIIs. The increased activation of the central ABA kinases was further supported by elevated levels of the two p-peptides corresponding to SnRK2III-activated group A bZIPs in mutant dry *dog1-1* seeds (fig. S5), despite the fact that these transcription factors are down-regulated in this mutant (fig. S2E) (*42*). SnRK2III deactivation follows a two-step mechanism whereby the conserved Trp-lock residue of PP2CAs is inserted into the kinase catalytic cleft after activation loop dephosphorylation to blunt basal activity and prevent auto- or trans-reactivation of SnRK2 isoforms (*37*). The absence of the Trp-lock residue is a key feature of AHG1 and its orthologs in monocots (fig. S6, A and B). Molecular modeling suggests that the valine residue present at this position in AHG1 cannot occupy the kinase active site as the tryptophan of other PP2CAs (fig. S6C). This limitation might explain previous observations that AHG1 is less effective than other PP2CAs in suppressing SnRK2.6 activity in vitro and that AHG1 is incapable of impairing SnRK2-mediated ABA responses using an in vivo reconstituted system (*30*, *43*, *44*). ABA levels were previously shown to be lower in dry seeds of *dog1-1* compared to NIL-DOG1 (*13*), but consistently with an increased SnRKIIIs activation, we found an upregulation of ABA receptors from subclasses I and II (Fig. 2G), which inhibit canonical PP2CAs in the absence or at low concentrations of ABA (*44*, *45*). Together, our data show that the ABA core signaling machinery is fully functional in *dog1-1* mutant seeds through increase of sensitization, priming of SnRK2III activity, activation of direct downstream effectors, and retained physiological seed stress responses. Yet, this molecular priming does not result in stable ABA responses at the end of maturation (fig. S2), nor does it override the nondormant phenotype of *dog1-1* (Fig. 1B). Consequently, in stark contrast to the current model, our data provide strong evidence that DOG1 function is not to regulate SnRK2III activation through the inhibition of AHG1 and thus that DOG1 controls dormancy independently of the central ABA kinase hub.

We noted that p-peptides from AFP1 and AFP2, with a conserved modification site, showed reduced abundances in *dog1-1* compared to NIL-DOG1 seeds (table S2). At this position, AFP1 exhibited approximately four times less phosphorylation in *dog1-1* compared to NIL-DOG1 dry seeds (Fig. 3C), prompting us to explore AFPs as critical targets of the DOG1-PP2C module to control dormancy. Only AFP2 was proposed to participate in dormancy so far (*46*, *47*). Here, we show that AFP1, AFP2, and AFP3 function as genetically highly redundant negative regulators of seed dormancy sensu stricto since the cumulation of their mutant alleles gradually enhanced this trait (figs. S9, A to C, and S14B). AHG1 is the only PP2CA interacting with AFPs in vivo (Fig. 3D and fig. S12), and we showed that AHG1 can dephosphorylate in vitro the p-sites regulated in *dog1-1*: AFP1{pS}115 and AFP2 {pS}112 (Fig. 3E and fig. S13). We demonstrated that AFP2 requires AHG1 to release dormancy (Fig. 3F). Coherently with AFPs-AHG1 genuine interaction, we only found a marginal effect of the *ahg3* mutant allele on the dormancy phenotype of transgenic *AFP2* seeds (Fig. 3F). This suggests that AHG1 governs the upstream activation of AFPs in part through dephosphorylation of a conserved B-domain residue. An inhibitory role of phosphorylation on AFP is further supported by

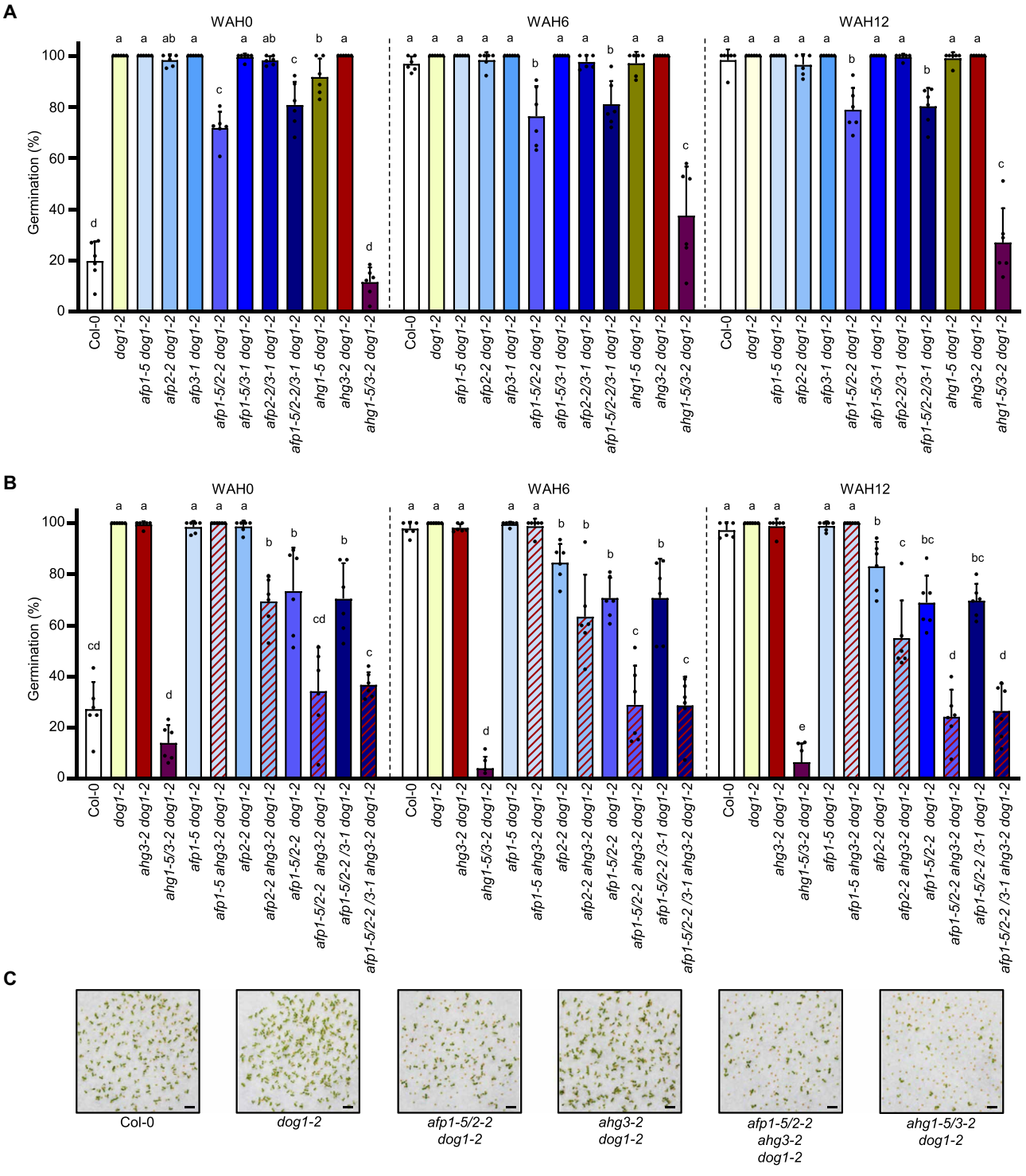


**Fig. 4. AFPs are required by the DOG1-PP2C module and operate specifically downstream of AHG1 in the control of seed dormancy.** (**A**) Germination capacity of single and multiple *afps* mutants in a *dog1-2* or (**B**) an *ahg3-2 dog1-2* genetic background at harvest, 6 and 12 weeks after harvest (WAH) (means ± SD, $n = 6$ biological replicates). Letters on the top of the bars indicate significantly different groups using a one-way ANOVA with a Tukey post hoc test ($\alpha = 0.05$). (**C**) Representative pictures showing the germination capacity of key combinatorial mutants after 32 WAH resuming the importance of AFP1 and AFP2 for the control of germination by the AHG1-related branch of the DOG1-PP2C module. Scale bars represent 2 mm.

the fact that the kinase SnRK1α1 antagonizes the effect of transient *AFP2* expression in *N. benthamiana* leaves (*48*).

AFP activities are relevant for the DOG1 pathway since *afp1* and *afp2* mutations partially revert the *dog1* dormancy phenotype (Fig. 4A and fig. S14B). Analysis of higher-order combinatorial mutants, including *afps*, *ahg3*, and *dog1* loss-of-function alleles, demonstrated that the contribution of the *ahg1* allele in the highly dormant *ahg1-5/3-2 dog1-2* mutant can largely be substituted by *afp1* and *afp2* mutations (Fig. 4, B and C). This result confirms AFP-independent functions for AHG3 and validates genetically that AFP1 and AFP2 are pivotal and genuine targets of AHG1 crucial for the DOG1-PP2C module to control seed dormancy. Pharmacological assays to manipulate ABA dynamics at imbibition suggest that AFP's function in the control of germination is independent of ABA levels (figs. S9D and S10C). This aligns with the reported extreme seed ABA insensitivity of constitutive *YFP:AFP2* overexpression lines used in this study (*38*, *39*). In conclusion, on the basis of converging lines of proteomic data, in vivo specific interactions, in vitro assays, as well as functional genetic and physiological evidence, we propose that AFPs are key molecular players in the DOG1 signaling pathway, acting downstream of AHG1.

AFPs are proteins of unknown function. ABA promotes the accumulation of AFP1 and AFP2, but they rapidly decline through protein posttranslational modification and proteasome-dependent mechanisms under stress-free conditions (*39*, *46*, *49*). Thus, they act as a rheostat transiently generated by ABA to moderate the magnitude of ABA responses or terminate them after stress relief (*50*). DOG1 protein remains stable in dry and imbibed seeds, regardless of the imbibition outcomes, but it is modified during dry storage and seed water uptake, suggesting that DOG1 has lost its activity in after-ripened seeds (*13*). De novo production of *DOG1* expression even as short as 3 hours after seed imbibition, through transgenic-inducible expression, does not prevent germination of freshly harvested *dog1-1* seeds (*13*). This supports the fact that the amount of active DOG1 protein readily present at early imbibition determines whether a seed is dormant or not. This indicates that the impact of DOG1 on the control of germination is limited to a narrow time window following water uptake and inefficient at later imbibitional stages of nondormant seeds in agreement with its irrelevance in the process to stop germination if stress conditions are met during imbibition.

The mode of action for DOG1 signaling presented here significantly expands our understanding of the molecular tinkering of ABA responses that allow seeds to accommodate germination time and stress reactiveness. We propose a nonconflicting bimodal molecular system for the mediation of ABA responses during seed imbibition by DOG1 and ABA (Fig. 5). DOG1 prevents AHG1 from promoting AFP-mediated shut-down of maturation-imposed ABA responses, thereby maintaining dormancy regardless of the initial drop of ABA levels upon imbibition. Because the DOG1-PP2C module functions are separated from the regulation of SnRK2III activity, it keeps ABA signaling primed independently of dormancy depth. This allows nondormant seeds to reinduce ABA responses and arrest germination upon sensing stress quickly and cost-efficiently. This dual molecular system allows seeds to bypass trade-offs between growth promotion and stress tolerance and to precisely adjust their dormancy level with minimal impact on their ability to withstand adverse conditions.

While further studies will be required to fully understand the detailed molecular mechanisms underlying this pathway and to explore the additional roles of PP2CA family members, in the regulation of seed dormancy, we report here the fundamental architecture of a dual molecular system governing ABA responses in the context of seed dormancy.

Germination timing is crucial to synchronize growth potential with seasonally fluctuating ambient conditions, thus vital for the successful establishment of seed plants in nature. The initial stages of plant domestication witnessed a strategic shift in resource allocation, diverting focus from the "fitness package" toward enhancing yield. Notably, cereal domestication marked a pivotal moment with the deliberate selection of genotypes lacking dormancy, ensuring swift and uniform germination across expansive fields (*51*). Beyond the induction of major issues like preharvest sprouting and varying malting quality, the loss of genetic diversity associated with the domestication of dormancy has reduced global plant fitness through selective sweeps at and around loci involved in ABA metabolism, causing pleiotropic effects (*52*–*55*). This highlights the need to neodomesticate the dormancy trait for the creation of "wild-relative-like" genetic restorer lines that maintain high fitness while keeping germination characteristics adapted to our food production system. DOG1 function is conserved in higher plants, the existence of the DOG1-PP2C module has been documented in crop species, and AFP function in the control of dormancy has been reported in wheat (TaAFP-B) and rice [mediator of OsbZIP46 deactivation and degradation (OsMODD)] (*56*–*61*). The genetic edition of OsMODD has recently been shown promising for the generation of rice restorer lines (*61*). The typical sequence feature of AHG1 and the modification of AFP the B-domain conserved serine residues by phosphorylation we described in *Arabidopsis* also exist in these major crop species (figs. S5, A and B, and S6D). While the evolutionary origin of the DOG1 signaling pathway presented herein is still to be defined, it appears largely conserved in seed plants. Through the mapping of a pathway controlling dormancy independently of other ABA-related germination traits, our findings offer so far unexplored opportunities for breeding programs aiming to deliver chemical-free solutions for contemporary environmental and food security challenges.

## MATERIALS AND METHODS

### Plant material, growth conditions, and seed batch productions

Seeds of *Arabidopsis thaliana* (L.) Heynh were used in this study. The Near Isogenic Line NIL-DOG1, which contains the *DOG1* QTL from Cape Verde Island in a *Landsberg erecta* (Ler) background, *dog1-1* (in NIL-DOG1 background), *dog1-2* (in Col-0 background), *abi2-1* (in Ler background) Ethyl Methanesulfonate (EMS) null mutants, or the transferred DNA (T-DNA) insertion null single mutant *ahg1-5* (SALK_049885) *ahg3-2* (SALK_028132), as well as the double *ahg1-5 ahg3-2* or triple *ahg1-5 ahg3-2 dog1-2*, were previously described (*13*, *20*, *26*, *62*). The *abi5-7* and *snrk2.2/3/6* mutant used as controls were previously described (*10*, *63*). The *afp1-3* (SALK_064533) *afp1-4* (SALK_098122C), *afp1-5* (SALK_020158C), *afp1-6* (SALK_005054) *afp2-1* (SALK_131676), *afp2-2* (SALK_145086C), *afp3-1* (SALK_037555), *afp3-2* (SALK_052114C), and *afp4-2* (SALK_208284C) are in the Col-0 background and were obtained from the Nottingham Arabidopsis Stock Centre (NASC) collection

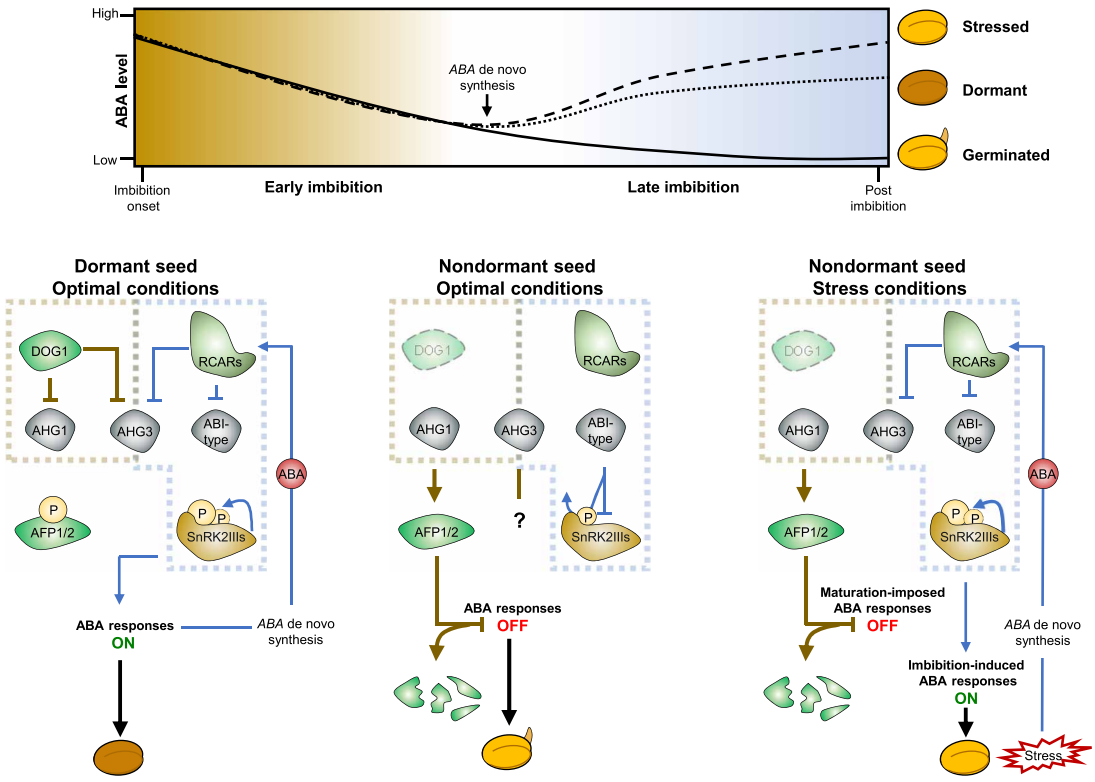


**Fig. 5. Proposed model for the accommodation of both dormancy and stress reactiveness during seed imbibition by a bimodular control of ABA responses.** Schematic representation of ABA dynamics (**top**) and the DOG1-PP2C module's operation alongside ABA core signaling in dormant (**bottom left**), nondormant unstressed (**bottom middle**), and nondormant stressed seeds (**bottom right**) during imbibition. ABA levels decrease upon imbibition regardless of the seed's stress or dormancy status. However, in dormant and stressed seeds, ABA is de novo synthesized at later imbibition stages to prevent sprouting after prolonged hydration. In dormant seeds imbibed under optimal conditions, DOG1 is active, inhibiting AFP activation by AHG1 and maintaining maturation-imposed ABA responses, independent of the early ABA drop. In later stages, active seed maturation responses induce ABA de novo synthesis, which, alongside the priming of SnRK2III activation, sustain ABA responses post-imbibition and prevent germination. In nondormant seeds (e.g., after-ripened or *dog1* mutants) imbibed under optimal conditions, DOG1 is inactive (dashed border; shaded), restoring AHG1 and AHG3 functions. AHG1 dephosphorylates AFP1 and AFP2, switching off ABA responses from maturation and leading to AFP disposal in the absence of stress during early imbibition. This disruption of ABA responses, combined with insufficient ABA de novo synthesis in a stress-free environment, promotes germination and growth. In nondormant seeds imbibed under stress, DOG1 remains inactive, activating AFP and destabilizing ABA responses from maturation. While SnRK2III activation remains primed (in *dog1* mutants, the activating phosphorylation mark is preserved), high ABA levels from stress-induced de novo synthesis at later imbibition stages prevent PP2CA-mediated SnRKIII repression, rapidly reactivating kinases and triggering ABA responses that halt germination. The question mark indicates unknown, AFP-independent AHG3 functions in germination control. Molecular events during early or late imbibition are shown as brown or blue connectors, respectively, with the DOG1-PP2C module (brown) and ABA core signaling pathway (blue) boxed.

(data S1). Homozygous *afp* single mutants were isolated using allele-specific primers (table S3). The expression of *AFP* full-length mRNA was investigated by reverse transcription polymerase chain reaction (RT-PCR), and no corresponding transcript was amplified for *afp1-5*, *afp2-2*, and *afp4-2*. The expression of *AFP1*, *AFP2*, and *AFP3* was reduced in *afp1-4*, *afp2-1*, and *afp3-1* but not changed in *afp1-3/afp1-6* and *afp3-2* compared to WT (fig. S16). Consequently, we considered *afp1-5*, *afp2-2*, and *afp4-2* as knockout and *afp1-4* or *afp2-1* as knockdown alleles. Multiple mutants were obtained by crossing, and homozygous lines were selected from self-pollinated F2 progenies using gene specific primers for the T-DNA insertion mutant and a Cleaved Amplified Polymorphic Sequence (CAPS) marker for the *dog1-2* allele (tables S3 and 4 and data S1). The hemizygous *35S::YFP:AFP2* (+/−) line expressing full-length AFP2 fused to YFP in its N terminus was a gift from R. Finkelstein and corresponds to the previously described 4A2 line (*38*, *39*). Homozygous *YFP:AFP2* overexpressing seeds fail to complete maturation and are shrunken and nonviable impeding the physiological characterization of *35S::YFP:AFP2* (+/+) progenies (*38*). Hemizygous *35S::YFP:AFP2* (+/−) in *ahg1-5* or *ahg3-2* backgrounds were obtained by crossing, and homozygous *ahg* single mutants harboring the *AFP2* transgene at the hemizygous state were selected from self-pollinated F2 progenies using alleles or transgene-specific primers (tables S3 and S4).

To produce seed batches for germination experiments, plants were cultivated on soil in a growth chamber with fluorescent light tubes with a 16-hour day (150 µE $m^{-2}$ $s^{-1}$), 8-hour night cycle at 50% Relative Humidity (RH). Except when stated otherwise, growing temperature for plant lines in the Col-0 ecotype was set at 21°/18°C (day/night) until bolting and lowered to 16°/14 °C during seed production and maturation to enhance seed dormancy at harvest (*64*). NIL-DOG1, *dog1-1* seed batches were matured at 21°/18°C.

Seeds were harvested when approximately two-third of the siliques turned brown by gently shaking the floral stem in paper bags

to avoid inclusion of seeds from immature siliques. Biological replicates were defined as the progenies of a single mother plant. Non-seed contaminants were removed through sieving on a 355-µm mesh, and nonfilled (aborted/undeveloped) seeds were mechanically sorted out by rolling seeds on paper several times. This treatment removed most of the black, wrinkled, and nonviable seeds from *35S::YFP-AFP2* (+/−) progenies. Consequently, the proportion of transgenic genotypes in seed batches from *35S::YFP-AFP2* (+/−) progenies is expected to be around 66% hemizygous and 33% WT. Processed seed batches were equilibrated for 7 days in a container fixed at 21°C and 50% HR before the start of the experiments (WAH0) and stored under these conditions during the full after-ripening kinetics.

### Germination assays

For each genotype, approximately 50 seeds per biological replicate were sown on filter paper (Whatman grade 1) moistened with double-distilled water in petri dishes. Seed plates were incubated under optimal conditions for *Arabidopsis* germination: in a transparent container fixed at 99% RH which was placed inside a growth chamber with fluorescent light tubes with a 16-hour day (80 µE $m^{-2}$ $s^{-1}$)/8-hour night cycle and a constant temperature of 22°C. To follow dormancy alleviation through after-ripening, seed batches were sown at regular intervals along storage in fixed condition of 22°C and 55% RH. The full viability of seed batches produced in our conditions for each genotype was verified by imbibing seeds in the presence of 50 µM gibberellic acid ($GA_{4+7}$) followed by a 48-hour stratification treatment before transfer to germination conditions (fig. S17). Fluridone and ABZ-E3M were used to manipulate the endogenous ABA level at imbibition (*65*, *66*). Stock solutions of fluridone, ABZ-E3M, ABA, and GA were dissolved in dimethyl sulfoxide (DMSO; final concentrations in the assays were 0.05%). When imbibed on chemicals, the mock control corresponds to 0.05% DMSO in water. When imbibed on ABA, seeds were submitted to a 48-hour stratification treatment before transfer to germination conditions. Germination per se (radicle emergence) was scored after 7 days of incubation in fixed conditions of 22°C and 55% RH. Raw germination data are available in data S2.

### Transcript analysis

Total RNA was extracted from 25 mg dry seeds using the RNAqueous Total RNA Isolation Kit (Invitrogen Thermo Fisher Scientific, Germany) as previously described (*13*). Samples were treated with a DNA-free kit (Invitrogen Thermo Fisher Scientific, Germany), and 1 µg per RNA sample was used for reverse transcription using the FastGene Scriptase II kit (Nippon Genetics EUROPE GmbH, Germany). Quantitative PCRs were performed using iQ SYBR Green Supermix in a CFX Connect Real-Time PCR Detection System (Bio-Rad Laboratories Inc., USA) as previously described (*67*). *PEX4* was used in all RT–quantitative PCR and *TIP41* and *UBI10* in semiquantitative PCR experiments as a validated internal housekeeping gene control for seed transcriptomic analysis (*42*). (Semi)-quantitative PCR primer sequences are available in table S5. Raw data are available in data S3.

### Protein extractions

*Arabidopsis* seeds or tobacco leaf samples were ground in liquid nitrogen with a mortar and pestle. Total proteins were solubilized in a buffer containing 50 mM Hepes (pH 7.5), 2.5% (w/v) SDS, and 5 mM dithiothreitol (DTT) under constant shaking at room temperature. Native protein complexes from tobacco leaves were solubilized in a buffer containing 50 mM tris-HCl (pH 7.9), 100 mM NaCl, 0.25 mM $MgCl_2$, 17.5% glycerol, 1 mM ascorbate, 5 mM DTT, 2.5% CHAPS, 2 mM phenylmethylsulfonyl fluoride, 20 µM MG132, macerozyme (1 U $ml^{-1}$; Boehringer Ingelheim, Germany), deoxyribonuclease I (DNase I; 50 U $ml^{-1;}$ Roche, Switzerland), and 1% (v/v) of plant protease inhibitor cocktail (Sigma-Aldrich, Germany) under constant shaking in an ice bath for 40 min. Protein extracts were clarified by repeated centrifugation until debris and oil free samples were obtained. Protein concentrations in the extracts were quantified using the Pierce 660-nm Protein Assay Reagent kit (Thermo Fisher Scientific, Germany) against a bovine serum albumin (BSA) standard dilution curve and directly used for downstream applications.

### Protein gel and immunodetection methods

Total (10 to 30 µg) or purified (0.5 to 2 µg) proteins were separated by SDS–polyacrylamide gel electrophoresis (SDS-PAGE) using homemade 10 to 12% (w/v) acrylamide/bis-acrylamide matrix. For Western blots, proteins were transferred on nitrocellulose membranes (Protran 0.2 µM nitrocellulose; Amersham Biosciences, UK) using Bjerrum-Schaefer-Nielsen buffer [48 mM tris, 39 mM glycine, and 15% methanol (pH 9.2)] via semidry transfer. After transfer, proteins were stained with Ponceau S before blocking with 3% BSA for 1 hour at room temperature (°C). Primary and secondary antibodies were incubated for 1 hour at room temperature (°C) or overnight at 4°C. Detection was performed using SuperSignal West Femto Maximum Sensitivity (Thermo Fisher Scientific) and a Chemidoc XP (Bio-Rad) or an Odyssey (LI-COR) imagining system. Primary and secondary antibodies and corresponding working dilutions used in this study are available in tables S6 and S7. Full-scan images for every Western blot membrane and protein gel presented in this study are available in data S4.

### Gene constructs

Full-length coding DNA sequences (CDS) for *AFP1*, *AFP2*, *AFP3*, *AFP4*, *ABI1*, *HAB1*, *HAB2*, *HAI1*, *HAI2*, *HAI3*, *SnRK2.6*, and *SnRK1a1* were amplified from cDNA of dry Col-0 seeds using gene-specific primers including the stop codon and cloned into pDONR201 or 207 using Bacterial Plasmid (BP) recombination reaction (Invitrogen) as previously described (*26*). The pDONOR entry clones for *AHG1*, *AHG3*, and *ABI2* were previously described (*26*). The $AHG1_{D123\_149A}$ inactive variant was obtained using the QuikChange II XL Site-Directed Mutagenesis Kit (Agilent). Primer sequences are available in table S8. Correct sequences were verified by Sanger sequencing at Microsynth SeqLab. pDONR entry clones were recombined into destination vectors using Ligation-Dependent Recombination (LR) reaction (Invitrogen, USA).

### Generation of *35S:YFP:SnRK2.6* transgenic lines

The CDS (including stop codon) of *SnRK2.6* was recombined from entry clones in the pEarleyGate104 vector (*68*) and transfected into *Agrobacterium tumefaciens* GV3101 pMP90 using electroporation before transformation of NIL-DOG1 and *dog1-1* using a floral-dipping method as described in (*67*). Homozygous single insertion lines were selected at the T3 generation through their resistance to phosphinothricin and genotyping by PCR. Two independent lines in each background were isolated (lines 1 and 2 are in NIL-DOG1 and lines 3 and 4 are in *dog1-1*). Further comparative assays used lines 2 and 4 based on a similar accumulation of the fusion protein in dry seed.

### Dissection of *A. thaliana* embryos and localization analysis

Six or 24 hours imbibed seeds in double-distilled water ($ddH_2O$) were transferred onto a glass plates, and intact embryos were isolated manually from surrounding tissue under a binocular as described in (*69*). Embryos were transferred onto microscope glass slides in water, for localization analyses using a Leica SP8 confocal microscope (Leica Microsystems, Mannheim, Germany) via a 63× water objective. YFP was excited at 514 nm with an argon laser, and emission was detected between 525 and 545 nm using a HyD detector. Imaging was conducted using the following settings: format, 1024 × 1024; bidirectional scan, 400 Hz; pinhole of 1 airy unit; digital zoom, 1 to 3.

### SnRK2.6 purification from dry seed and kinase assays

Proteins were extracted from 50-mg dry seed material as stated above with the following modification: Proteins were suspended in 1 ml of ice-cold extraction buffer [50 mM Hepes (pH 7.5), 150 mM NaCl, 10 μM adenosine triphosphate (ATP), 1% (w/v) Triton X-100, 5 mM DTT, 1 mM EGTA, 1 mM EDTA, DNase I (50 U/ml), macerozyme (1 U/ml), 20 mM β-glycerophosphate, 50 mM Natriumfluorid (NaF), 1 mM $Na_3VO_4$, 1% plant protease inhibitor cocktail, 20 μM MG132, and 50 μM ABA], and samples were vortexed and incubated for 10 min at room temperature under gentle shaking before clarification by centrifugation. After quantification, the total protein amount was normalized to 0.75 mg/ml. For each assay, 25 μl of agarose beads coupled to a green fluorescent protein (GFP) antibody (GFP-Trap, ChromoTek) corresponding to 10 μg of GFP-binding capacity was equilibrated three times in 50 mM Hepes (pH 7.5), 150 mM NaCl, 5 mM DTT, 1 mM EGTA, and 1 mM EDTA. One milligram of the total protein was mixed with beads followed by incubation under constant rotation for 2 hours at 4°C. After centrifugation (200*g* for 1 min), beads were washed twice with 500 μl of equilibration buffer, and a last wash was performed using the kinase buffer [50 mM Hepes (pH 7.5), 1 mM EGTA, 10 mM $MgCl_2$, 1 mM DTT, and 20 mM β-glycerophosphate]. After the last centrifugation step, the supernatant was discarded, and the beads were resuspended in 50 μl (final volume) of kinase buffer. A 15-μl aliquot was mixed with 15 μl of 2× Laemmli buffer [4× stock: 1% SDS, 10% glycerol, 0.005% bromophenol blue, 62.5 mM tris-HCl (pH 6.8), and 355 mM 2-mercaptoethanol] and used for Western blot analyses. The residual 35 μl were mixed with 15 μl kinase buffer and the reaction was started by addition of 1.5 μl NaCl (150 mM), MBP 1.5 μl (10 mg/ml), 0.15 μl ATP (10 mM), 2 μCi $^{32}P$ γ-ATP. After 1-hour incubation at room temperature (°C), the reaction was stopped by addition of 15 μl of 4× Laemmli buffer before SDS-PAGE separation. Gels were stained and fixed using Coomassie staining solution and placed in an exposure cassette with a phosphor screen for 1 hour. The incorporation of $^{32}P$ into the MBP substrate was analyzed using a Typhoon$^{T}$ FLA700 Scanner (GE Healthcare). The images were taken using the phosphorimaging mode, at a pixel size of 25 μm and a latitude of 4. The voltage, which was applied to the photomultiplier tube, was set at 750 V. Full-scan images of autoradiogram and total staining are available in data S4.

### Yeast two-hybrid assay

The CDS (including stop codon) of *AFP1*, *AFP2*, *AFP3*, *AFP4*, *SnRK2.6*, *ABI1*, *HAB1*, *HAB2*, *HAI1*, *HAI2*, and *HAI3* were recombined from entry clones in the pAS2-gateway (GAL4 BD fusion) and pACT2-gateway (GAL4 AD fusion) vectors (modified from Clontech), respectively. pACT2:AHG1 pACT2:AHG3 and pACT2:ABI2 were previously described (*26*). Interaction assays were performed in the yeast strain PJ69-4alpha as previously described (*26*). Interactions were monitored via drop tests on −LWH medium (−LWH) lacking L, W, and His (H) with 5 and 10 mM 3-aminotriazole in dilutions of $10^{-1}$, $10^{-2}$, and $10^{-3}$. Yeast was grown at 30°C, and photos were recorded after 2 or 4 days for −LW or −LWH plates, respectively.

### Tobacco leaf transient transformation

Electrocompetent *A. tumefaciens* GV3101 (pMP90) cells were transformed with binary destination vectors and grown at 28°C (*70*). Overnight cultures inoculated with single colonies were cultivated under constant shaking at 28°C. Bacteria were diluted to a final $OD_{600}$ (optical density at 600 nm) of 0.5 in activation medium for tobacco infiltration [10 mM $MgCl_2$, 10 mM MES (pH 5.7), and 100 μM acetosyringone] and mixed with the p19 helper strain at an $OD_{600}$ of 0.4 (*71*). Four-week-old *N. benthamiana* leaves were infiltrated with a syringe.

### Coimmunoprecipitation

The full-length CDS (including stop) of *AFP1*, *AFP2*, *AFP3*, *AFP4*, *SnRK2.6*, and *SnRK1a1* were recombined from entry clones in the pBat-TL-Venus-GW (gift from P. Känel, Fraunhofer IME, Münster, Germany) vector, while *AHG1*, *AHG3*, and *ABI2* were recombined in the pAlligator2 vector (*72*). Recombined vectors were used for tobacco coinfiltration, and native protein complexes were purified from 48-hour infiltrated leaves. For each pull-down, 25 μl of agarose beads coupled to a GFP antibody (GFP-Trap, ChromoTek) was equilibrated in a buffer containing 50 mM tris-HCl (pH 7.9), 100 mM NaCl, 0.25 mM $MgCl_2$, 17.5% glycerol, 1 mM ascorbate, and 5 mM DTT. Equilibrated beads were dispensed in 2 ml of native extract containing 3 mg of protein and incubated under rotation at 4°C for 45 min. After incubation, beads were separated from nonbound fractions by centrifugation and washed three times with 500 μl of equilibration buffer. Bound protein complexes were eluted from the beads by adding of 4× Laemmli buffer, followed by 5-min incubation at room temperature (°C). Samples were diluted four times with $ddH_2O$ and boiled at 95°C before SDS-PAGE separation. For each interaction paring, input and elution fraction were analyzed on a single membrane. Venus (Bait) fusion proteins were detected using anti-GFP antibody. After stripping of membranes, 3xHA (prey) fusion proteins were detected on the same membrane using anti–hemagglutinin (HA) antibody. The Ponceau S staining was used as a loading control to control the quality of the Venus-tagged fusion protein enrichment (ratio signal anti-GFP/RbcL).

### Production and purification of recombinant protein

Preparation of recombinant 6xHIS:MBP:AHG1 and 6xHIS:MBP:-$AHG1_{D123\_149A}$ was performed as previously described (*26*). The purity and the specific activity toward the enzymes used in this study were followed by SDS-PAGE and using the RRA{pT}VA standard peptide, respectively (fig. S12A).

### In vitro phosphatase assays

The RRA{pT}VA standard peptide was obtained from Promega (V248A). Synthetic phosphorylated peptides of 14 amino acids from AFP1 modified at S115 (GLMRTT{pS}LPAESEE), AFP2 modified at S112 (GLERTT{pS}LPAEMEE), and SnRK2IIIs modified at a conserved serine corresponding to S171 in SnRK2.6 (KSSVLH{pS}QPKSTVG) were obtained from Biomatik LLC (USA). Reactions

were performed in flat-bottom 96-well plates in a final volume of 50 µl. The phosphatase reactions were started by addition of 4.4 µM recombinant 6xHIS:MBP:AHG1 or 6xHIS:MBP:AHG1$_{D123_149A}$ proteins in the reaction mix containing 50 mM Hepes buffer (pH 7.5) and 10 mM $MgCl_2$ and the indicated concentration of the corresponding substrate peptide. Reactions were performed for 5 to 30 min at room temperature and stopped by addition of 100 µl of BIOMOL Green (Enzo Life Sciences Inc., Germany). The dye was developed for 30 min at room temperature before measuring the absorbance at 630 nm in a Tecan Infinite M200 Pro plate reader (Tecan Group, Switzerland). Specific activities were calculated using a serial dilution of free phosphate as standard. As positive control for the dephosphorylation of the SnRK2III peptide, a reaction was performed using 0.07 µM commercial calf intestinal alkaline phosphatase (Thermo Fisher Scientific, Germany). Raw activity data are available in data S5.

### Proteolytic digestion

Total protein extracts form NIL-DOG1 or *dog1-1* dry or 6-hour imbibed seeds were digested to peptides using the Filter Aided Sample Preparation method (*73*, *74*). Proteins (1 mg) were diluted in 8 M urea in 0.1 M tris HCl (pH 8.5) (to a final volume of 1 ml) and reduced by addition of DTT at a final concentration of 10 mM for 1 hour at room temperature (°C). Cysteines were alkylated by addition of 2-Chloracetamid (CAA) at a final concentration of 45 mM and incubated for 1 hour in the dark at room temperature (°C). The excess of CAA was quenched by addition of DTT at a final concentration of 83 mM for 1 hour in the dark at room temperature (°C). The whole mixture was transferred on an Amicon 10-kDa centrifugation filter (Millipore, Darmstadt, Germany) and diluted three times with 50 mM ammonium bicarbonate (ABC) buffer. The volume was reduced to 500 µl by centrifugation at 3000*g* and further diluted six times with ABC buffer. The volume was further reduced to 250 µl by centrifugation, and proteins were digested by addition of 2 µg of trypsin (T6567, Sigma-Aldrich, Darmstadt, Germany) and incubation at 37°C overnight under agitation. Digested peptides were recovered in the flow-through by centrifugation. Concentrator filters were washed twice with 0.5 M NaCl followed by centrifugation. The flow through from wash fractions was combined with recovered peptides. For the targeted analysis of YFP:SnRK2.6 phosphorylation status, the sample were prepared as for the kinase assays with the following modification: The β-glycerophosphate was omitted in extraction buffer, and the last bead wash was performed with equilibration buffer. Elution was performed by incubating beads in 0.1% of trifluoroacetic acid (TFA) for 5 min before supernatant harvest and addition of an equal volume of neutralization buffer [8 M urea in 0.1 M tris-HCl (pH 8.5)]. Eluted proteins were reduced for 30 min in the dark by adding DTT at a final concentration of 12 mM and were subsequently alkylated for 1 hour in the dark by adding chloroacetamide at a final concentration of 44 mM. The excess of CAA was quenched for 30 min in the dark by adding DTT at a final concentration of 120 mM. The mixture was diluted seven times with ABC buffer, before addition of 1 µg trypsin and overnight incubation at 37°C.

### Mass spectrometry sample preparation

Peptides from total protein extracts were acidified by addition of formic acid at a final concentration of 0.5% and desalted using Sep-Pak SPE 1 cc/100 mg (Waters, Eschborn, Germany) as previously described (*75*). Ten micrograms of desalted peptides was processed for total proteome analysis by prefractionation in three fractions using Empore styrenedivenylbenzene reversed phase sulfonate material (3M) as previously described (*76*). Phosphopeptide enrichment from total protein extracts was performed by solving 400 µg of desalted peptides in 50% acetonitrile (ACN) and 1% TFA supplemented with 2,5-dihydroxybenzoic acid (20 mg/ml) and subjected to titanium dioxide ($TiO_2$) affinity chromatography using 6 mg of $TiO_2$ beads (5 mm; GL Sciences) per sample as previously described (*75*). Elution from $TiO_2$ or agarose coupled to a GFP antibody beads was further desalted with StageTips (Empore C18; 3M) as previously described (*77*). After desalting, peptide samples were dried in a centrifugal evaporator.

### LC-MS/MS data acquisition

Before measurement, peptides were resuspended in A* buffer (2% ACN and 0.1% TFA). Proteomic samples were measured by liquid chromatography–tandem mass spectrometry (LC-MS/MS) using data-dependent acquisition (DDA) on an EASY-nLC 1000 system (Thermo Fisher Scientific, Germany) coupled to an Orbitrap Q Exactive Plus mass spectrometer (Thermo Fisher Scientific, Germany) as previously described (*75*). For targeted analysis of YFP:SnRK2.6 phosphorylation status, the samples were split in two and measured on an EASY-nLC 1200 system (Thermo Fisher Scientific, Germany) coupled to an Orbitrap Exploris 480 mass spectrometer (Thermo Fisher Scientific, Germany) as previously described for DDA (*78*) and using the parallel reaction monitoring (PRM) mode targeting peptides summarized in table S9.

### MS data processing and analysis

Raw LC-MS/MS spectra were processed using MaxQuant (version 1.6.17.0) (http://maxquant.org/) against the Arabidopsis Araport11 database (*79*) with label-free quantification (LFQ) enabled (*80*). Common protein contaminant and decoy sequences were automatically added during the search. Trypsin cleavage specificity was required with a maximum of two missed cleavages allowed and a minimal peptide length of seven amino acids. Carbamidomethylation of cysteine residues was set as fixed, and oxidation of Met and protein N-terminal acetylation were set as variable modifications. For the analysis of phosphopeptide-enriched samples, phosphorylation of Ser, Thr, and Tyr was added as additional variable posttranslational modifications. The false discovery rate (FDR) cutoff was set at 1%. A total of 5004 *Arabidopsis* protein groups and 4848 unique p-peptides (FDR < 1%, score > 40, and δ score > 6) covering 1616 phosphorylation sites were quantified. MaxQuant output files were further analyzed using version 1.6.6.0 of Perseus (*81*). For both proteome and phosphoproteome measurements, the reproducibility between replicates for a given genotype and condition was very high as demonstrated by Pearson correlation coefficients calculated in Perseus (figs. S18 and S19). Protein LFQ intensities (total proteome analysis) or peptide intensities (phosphoproteome analysis) were $log_2$-transformed, and the data were filtered for valid values in at least two of the three replicates of one genotype in either dry or imbibed conditions. After filtering, 4324 protein groups and 984 phosphopeptides (for which the exact phosphorylated residues could be determined on 828 sites) were retained for statistical analysis. MS outcome metrics are available as table S1. Annotation for protein localization was performed in Perseus using the SUBA4 consensus database. Missing values were imputed from normal distribution using a width of ($log_2$) 0.5 or 0.6 and a downshift of ($log_2$) 2 or 1.95 for total proteomes or phosphoproteome datasets, respectively (fig.

S20). We used an empirical Bayes method to identify significant changes in protein or p-peptide abundance between genotype in dry or 6-hour imbibed seeds. Fold changes and *P* values were calculated using the LIMMA ("Linear Models for Microarray Data") package on R (*82*). Data analysis outcomes are available as data S6. GO was performed in Cytoscape using a hypergeometric test with a significance level of 0.05 after correction by a Benjamin and Hochberg FDR test in the BiNGO app (*83*, *84*). A seed dry or imbibed proteome obtained from the Arabidopsis Draft Proteome was used as a reference background set for GO analysis (*85*). Proteins annotated as implied in ABA responses were retrieved using the GO:009737 terms in Amigo2 database (https://amigo.geneontology.org/amigo). For targeted analysis of YFP:SnRK2.6 phosphorylation status, raw LC-MS/MS spectra from both acquisition methods (DDA and PRM) were processed together as separate parameter groups using the MaxQuant with the settings described above expected that LFQ quantification was disabled for PRM data. Localization probabilities were further manually filtered, retaining entries with a score superior to 60 to ensure high-confidence identification and localization. Data analysis outcomes are available as data S7.

### Protein sequence, phylogeny, and structures analyses

Protein amino acid sequence alignments and phylogenetic trees were performed in Mega11 using the ClustalOmega and the maximum likehood joining algorithms. Structures of *Arabidopsis* SnRK2.6 in complex with HAB1 were obtained from the Protein Data Bank repository (https://www.rcsb.org/) with the accession number 3UJG, and modeling of AHG1 was obtained from the AlphaFold repository (https://alphafold.ebi.ac.uk/). Superimposition of protein structures was performed using PDBeFold (https://ebi.ac.uk/msd-srv/ssm/). Visualization and analyses were performed using PyMOL software (DeLano Scientific LLC).

### Image and statistical analysis

Western blot, autoradiogram, and gel signal intensities were obtained by image densitometry analysis using ImageJ. Values and calculations are available in data S8. Differences in paired or unpaired comparison were tested using a Student's *t* test. For multiple comparisons, germination percentage values were arcsin square root transformed to accomplish the prerequisites of normality before applying a one-way analysis of variance (ANOVA) with a Tukey post hoc test. Tests were performed in the Origin2023 or R (version 4.3.1) software. Bar graphs were built in GraphPrism V10.2.1.

## Supplementary Materials

**The PDF file includes:**

Figs. S1 to S20
Tables S1 to S9
Legends for data S1 to S8
References

**Other Supplementary Material for this manuscript includes the following:**

Data S1 to S8

## REFERENCES AND NOTES


1. C. Baroux, U. Grossniklaus, "Chapter twenty-one - Seeds—An evolutionary innovation underlying reproductive success in flowering plants" in *Current Topics in Developmental Biology* (Academic Press, 2019), vol. 131, pp. 605–642.
2. J. de Vries, J. M. Archibald, Plant evolution: Landmarks on the path to terrestrial life. *New Phytol.* **217**, 1428–1434 (2018).
3. J. D. Bewley, M. Black, *Physiology and Biochemistry of Seeds in Relation to Germination: Volume 2: Viability, Dormancy, and Environmental Control* (Springer, 2012).
4. W. E. Finch-Savage, G. Leubner-Metzger, Seed dormancy and the control of germination. *New Phytol.* **171**, 501–523 (2006).
5. G. Née, Y. Xiang, W. J. J. Soppe, The release of dormancy, a wake-up call for seeds to germinate. *Curr. Opin. Plant Biol.* **35**, 8–14 (2017).
6. J. G. Pausas, B. B. Lamont, J. E. Keeley, W. J. Bond, Bet-hedging and best-bet strategies shape seed dormancy. *New Phytol.* **236**, 1232–1236 (2022).
7. R. Finkelstein, Abscisic acid synthesis and response. *Arabidopsis Book* **11**, e0166 (2013).
8. M. Koornneef, M. L. Jorna, D. L. C. Brinkhorst-van der Swan, C. M. Karssen, The isolation of abscisic acid (ABA) deficient mutants by selection of induced revertants in non-germinating gibberellin sensitive lines of *Arabidopsis thaliana* (L.) heynh. *Theor. Appl. Genet.* **61**, 385–393 (1982).
9. Y. Fujita, K. Nakashima, T. Yoshida, T. Katagiri, S. Kidokoro, N. Kanamori, T. Umezawa, M. Fujita, K. Maruyama, K. Ishiyama, M. Kobayashi, S. Nakasone, K. Yamada, T. Ito, K. Shinozaki, K. Yamaguchi-Shinozaki, Three SnRK2 protein kinases are the main positive regulators of abscisic acid signaling in response to water stress in arabidopsis. *Plant Cell Physiol.* **50**, 2123–2132 (2009).
10. H. Fujii, J.-K. Zhu, Arabidopsis mutant deficient in 3 abscisic acid-activated protein kinases reveals critical roles in growth, reproduction, and stress. *Proc. Natl. Acad Sci. U.S.A.* **106**, 8380–8385 (2009).
11. Y. Zhao, Z. Zhang, J. Gao, P. Wang, T. Hu, Z. Wang, Y.-J. Hou, Y. Wan, W. Liu, S. Xie, T. Lu, L. Xue, Y. Liu, A. P. Macho, W. A. Tao, R. A. Bressan, J.-K. Zhu, *Arabidopsis* duodecuple mutant of PYL ABA receptors reveals PYL repression of ABA-independent SnRK2 activity. *Cell Rep.* **23**, 3340–3351.e5 (2018).
12. S. Ali-Rachedi, D. Bouinot, M.-H. Wagner, M. Bonnet, B. Sotta, P. Grappin, M. Jullien, Changes in endogenous abscisic acid levels during dormancy release and maintenance of mature seeds: Studies with the Cape Verde Islands ecotype, the dormant model of *Arabidopsis thaliana*. *Planta* **219**, 479–488 (2004).
13. K. Nakabayashi, M. Bartsch, Y. Xiang, E. Miatton, S. Pellengahr, R. Yano, M. Seo, W. J. J. Soppe, The time required for dormancy release in Arabidopsis is determined by DELAY OF GERMINATION1 protein levels in freshly harvested seeds. *Plant Cell* **24**, 2826–2838 (2012).
14. V. Lefebvre, H. North, A. Frey, B. Sotta, M. Seo, M. Okamoto, E. Nambara, A. Marion-Poll, Functional analysis of Arabidopsis NCED6 and NCED9 genes indicates that ABA synthesized in the endosperm is involved in the induction of seed dormancy. *Plant J.* **45**, 309–319 (2006).
15. S. Toh, A. Imamura, A. Watanabe, K. Nakabayashi, M. Okamoto, Y. Jikumaru, A. Hanada, Y. Aso, K. Ishiyama, N. Tamura, S. Iuchi, M. Kobayashi, S. Yamaguchi, Y. Kamiya, E. Nambara, N. Kawakami, High temperature-induced abscisic acid biosynthesis and its role in the inhibition of gibberellin action in Arabidopsis seeds. *Plant Physiol.* **146**, 1368–1385 (2008).
16. N. Sano, A. Marion-Poll, ABA metabolism and homeostasis in seed dormancy and germination. *Int. J. Mol. Sci.* **22**, 5069 (2021).
17. S. Penfield, J. King, Towards a systems biology approach to understanding seed dormancy and germination. *Proc. R. Soc. B: Biol. Sci.* **276**, 3561–3569 (2009).
18. M. Iwasaki, S. Penfield, L. Lopez-Molina, Parental and environmental control of seed dormancy in *Arabidopsis thaliana*. *Annu. Rev. Plant Biol.* **73**, 355–378 (2022).
19. C. Alonso-Blanco, L. Bentsink, C. J. Hanhart, H. B. Vries, M. Koornneef, analysis of natural allelic variation at seed dormancy loci of *Arabidopsis thaliana*. *Genetics* **164**, 711–729 (2003).
20. L. Bentsink, J. Hanson, C. J. Hanhart, H. Blankestijn-De Vries, C. Coltrane, P. Keizer, M. El-Lithy, C. Alonso-Blanco, M. T. De Andrés, M. Reymond, F. Van Eeuwijk, S. Smeekens, M. Koornneef, Natural variation for seed dormancy in Arabidopsis is regulated by additive genetic and molecular pathways. *Proc. Natl. Acad. Sci. U.S.A.* **107**, 4264–4269 (2010).
21. M. Murphey, K. Kovach, T. Elnacash, H. He, L. Bentsink, K. Donohue, *DOG1*-imposed dormancy mediates germination responses to temperature cues. *Environ. Exp. Bot.* **112**, 33–43 (2015).
22. A. Martínez-Berdeja, M. C. Stitzer, M. A. Taylor, M. Okada, E. Ezcurra, D. E. Runcie, J. Schmitt, Functional variants of *DOG1* control seed chilling responses and variation in seasonal life-history strategies in *Arabidopsis thaliana*. *Proc. Natl. Acad. Sci. U.S.A.* **117**, 2526–2534 (2020).
23. I. Kronholm, F. X. Picó, C. Alonso-Blanco, J. Goudet, J. de Meaux, Genetic basis of adaptation in *Arabidopsis thaliana*: Local adaptation at the seed dormancy QTL DOG1. *Evolution* **66**, 2287–2302 (2012).
24. D. S. Vidigal, A. C. S. S. Marques, L. A. J. Willems, G. Buijs, B. Méndez-Vigo, H. W. M. Hilhorst, L. Bentsink, F. X. Picó, C. Alonso-Blanco, Altitudinal and climatic associations of seed dormancy and flowering traits evidence adaptation of annual life cycle timing in *Arabidopsis thaliana*. *Plant Cell Environ.* **39**, 1737–1748 (2016).
25. L. Bentsink, J. Jowett, C. J. Hanhart, M. Koornneef, Cloning of *DOG1* a quantitative trait locus controlling seed dormancy in Arabidopsis. *Proc. Natl. Acad. Sci. U.S.A.* **103**, 17042–17047 (2006).

26. G. Née, K. Kramer, K. Nakabayashi, B. Yuan, Y. Xiang, E. Miatton, I. Finkemeier, W. J. J. Soppe, DELAY of GERMINATION1 requires PP2C phosphatases of the ABA signalling pathway to control seed dormancy. *Nat. Commun.* **8**, 72 (2017).
27. N. Nishimura, T. Yoshida, N. Kitahata, T. Asami, K. Shinozaki, T. Hirayama, ABA-hypersensitive germination1 encodes a protein phosphatase 2C, an essential component of abscisic acid signaling in Arabidopsis seed. *Plant J.* **50**, 935–949 (2007).
28. G. Née, T. Krüger, Dry side of the core: A meta-analysis addressing the original nature of the ABA signalosome at the onset of seed imbibition. *Front. Plant. Sci.* **14**, 1192652 (2023).
29. N. Nishimura, W. Tsuchiya, J. J. Moresco, Y. Hayashi, K. Satoh, N. Kaiwa, T. Irisa, T. Kinoshita, J. I. Schroeder, J. R. Yates III, T. Hirayama, T. Yamazaki, Control of seed dormancy and germination by DOG1-AHG1 PP2C phosphatase complex via binding to heme. *Nat. Commun.* **9**, 2132 (2018).
30. T. Umezawa, N. Sugiyama, M. Mizoguchi, S. Hayashi, F. Myouga, K. Yamaguchi-Shinozaki, Y. Ishihama, T. Hirayama, K. Shinozaki, Type 2C protein phosphatases directly regulate abscisic acid-activated protein kinases in *Arabidopsis*. *Proc. Natl. Acad. Sci. U.S.A.* **106**, 17588–17593 (2009).
31. M. Okamoto, K. Tatematsu, A. Matsui, T. Morosawa, J. Ishida, M. Tanaka, T. A. Endo, Y. Mochizuki, T. Toyoda, Y. Kamiya, K. Shinozaki, E. Nambara, M. Seki, Genome-wide analysis of endogenous abscisic acid-mediated transcription in dry and imbibed seeds of Arabidopsis using tiling arrays. *Plant J.* **62**, 39–51 (2010).
32. S. Katsuta, G. Masuda, H. Bak, A. Shinozawa, Y. Kamiyama, T. Umezawa, D. Takezawa, I. Yotsui, T. Taji, Y. Sakata, Arabidopsis Raf-like kinases act as positive regulators of subclass III SnRK2 in osmostress signaling. *Plant J.* **103**, 634–644 (2020).
33. Y. Takahashi, J. Zhang, P. K. Hsu, P. H. O. Ceciliato, L. Zhang, G. Dubeaux, S. Munemasa, C. Ge, Y. Zhao, F. Hauser, J. I. Schroeder, MAP3Kinase-dependent SnRK2-kinase activation is required for abscisic acid signal transduction and rapid osmotic stress response. *Nat. Commun.* **11**, 12 (2020).
34. Z. Lin, Y. Li, Z. Zhang, X. Liu, C.-C. Hsu, Y. Du, T. Sang, C. Zhu, Y. Wang, V. Satheesh, P. Pratibha, Y. Zhao, C.-P. Song, W. A. Tao, J.-K. Zhu, P. Wang, A RAF-SnRK2 kinase cascade mediates early osmotic stress signaling in higher plants. *Nat. Commun.* **11**, 613 (2020).
35. N. Fàbregas, T. Yoshida, A. R. Fernie, Role of Raf-like kinases in SnRK2 activation and osmotic stress response in plants. *Nat. Commun.* **11**, 6184 (2020).
36. F. Yu, Y. Wu, Q. Xie, Precise protein post-translational modifications modulate ABI5 activity. *Trends Plant Sci.* **20**, 569–575 (2015).
37. F.-F. Soon, L.-M. Ng, X. E. Zhou, G. M. West, A. Kovach, M. H. E. Tan, K. M. Suino-Powell, Y. He, Y. Xu, M. J. Chalmers, J. S. Brunzelle, H. Zhang, H. Yang, H. Jiang, J. Li, E.-L. Yong, S. Cutler, J.-K. Zhu, P. R. Griffin, K. Melcher, H. E. Xu, Molecular mimicry regulates ABA signaling by SnRK2 kinases and PP2C phosphatases. *Science* **335**, 85–88 (2012).
38. T. J. Lynch, B. J. Erickson, D. R. Miller, R. R. Finkelstein, ABI5-binding proteins (AFPs) alter transcription of ABA-induced genes via a variety of interactions with chromatin modifiers. *Plant Mol. Biol.* **93**, 403–418 (2017).
39. T. Lynch, G. Née, A. Chu, T. Krüger, I. Finkemeier, R. R. Finkelstein, ABI5 binding protein2 inhibits ABA responses during germination without ABA-INSENSITIVE5 degradation. *Plant Physiol.* **189**, 666–678 (2022).
40. P. L. Rodriguez, J. Lozano-Juste, A. Albert, "Chapter Two - PYR/PYL/RCAR ABA receptors" in *Advances in Botanical Research* (Academic Press, 2019), vol. 92, pp. 51–82.
41. N. Sajeev, M. Koornneef, L. Bentsink, A commitment for life: Decades of unraveling the molecular mechanisms behind seed dormancy and germination. *Plant Cell* **36**, 1358–1376 (2024).
42. B. J. W. Dekkers, H. He, J. Hanson, L. A. J. Willems, D. C. L. Jamar, G. Cueff, L. Rajjou, H. W. M. Hilhorst, L. Bentsink, The Arabidopsis *Delay of Germination 1* gene affects Abscisic Acid Insensitive 5 (ABI5) expression and genetically interacts with ABI3 during Arabidopsis seed development. *Plant J.* **85**, 451–465 (2016).
43. R. Antoni, M. Gonzalez-Guzman, L. Rodriguez, A. Rodrigues, G. A. Pizzio, P. L. Rodriguez, Selective inhibition of clade A phosphatases type 2C by PYR/PYL/RCAR abscisic acid receptors. *Plant Physiol.* **158**, 970–980 (2012).
44. M. Ruschhaupt, J. Mergner, S. Mucha, M. Papacek, I. Doch, S. V. Tischer, D. Hemmler, D. Chiasson, K. H. Edel, J. Kudla, P. Schmitt-Kopplin, B. Kuster, E. Grill, Rebuilding core abscisic acid signaling pathways of Arabidopsis in yeast. *EMBO J.* **38**, e101859 (2019).
45. S. V. Tischer, C. Wunschel, M. Papacek, K. Kleigrewe, T. Hofmann, A. Christmann, E. Grill, Combinatorial interaction network of abscisic acid receptors and coreceptors from *Arabidopsis thaliana*. *Proc. Natl. Acad. Sci U.S.A.* **114**, 10280–10285 (2017).
46. M. E. Garcia, T. Lynch, J. Peeters, C. Snowden, R. Finkelstein, A small plant-specific protein family of ABI five binding proteins (AFPs) regulates stress response in germinating Arabidopsis seeds and seedlings. *Plant Mol. Biol.* **67**, 643–658 (2008).
47. G. Deng, H. Sun, Y. Hu, Y. Yang, P. Li, Y. Chen, Y. Zhu, Y. Zhou, J. Huang, S. J. Neill, X. Hu, A transcription factor WRKY36 interacts with AFP2 to break primary seed dormancy by progressively silencing *DOG1* in Arabidopsis. *New Phytol.* **238**, 688–704 (2023).
48. C. S. Carianopol, S. Gazzarrini, SnRK1α1 antagonizes cell death induced by transient overexpression of *Arabidopsis thaliana* ABI5 Binding Protein 2 (AFP2). *Front. Plant Sci.* **11**, 582208 (2020).
49. L. Lopez-Molina, S. Mongrand, N. Kinoshita, N.-H. Chua, AFP is a novel negative regulator of ABA signaling that promotes ABI5 protein degradation. *Genes Dev.* **17**, 410–418 (2003).
50. Y. Vittozzi, T. Krüger, A. Majee, G. Née, S. Wenkel, ABI5 binding proteins: Key players in coordinating plant growth and development. *Trends Plant Sci.* **29**, 1006–1017 (2024).
51. R. N. Spengler III, Anthropogenic seed dispersal: Rethinking the origins of plant domestication. *Trends Plant Sci.* **25**, 340–348 (2020).
52. M. Wang, W. Li, C. Fang, F. Xu, Y. Liu, Z. Wang, R. Yang, M. Zhang, S. Liu, S. Lu, T. Lin, J. Tang, Y. Wang, H. Wang, H. Lin, B. Zhu, M. Chen, F. Kong, B. Liu, D. Zeng, S. A. Jackson, C. Chu, Z. Tian, Parallel selection on a dormancy gene during domestication of crops from multiple families. *Nat. Genet.* **50**, 1435–1441 (2018).
53. X. Xu, X. Liu, S. Ge, J. D. Jensen, F. Hu, X. Li, Y. Dong, R. N. Gutenkunst, L. Fang, L. Huang, J. Li, W. He, G. Zhang, X. Zheng, F. Zhang, Y. Li, C. Yu, K. Kristiansen, X. Zhang, J. Wang, M. Wright, S. McCouch, R. Nielsen, J. Wang, W. Wang, Resequencing 50 accessions of cultivated and wild rice yields markers for identifying agronomically important genes. *Nat. Biotechnol.* **30**, 105–111 (2012).
54. M. B. Hufford, X. Xu, J. van Heerwaarden, T. Pyhäjärvi, J.-M. Chia, R. A. Cartwright, R. J. Elshire, J. C. Glaubitz, K. E. Guill, S. M. Kaeppler, J. Lai, P. L. Morrell, L. M. Shannon, C. Song, N. M. Springer, R. A. Swanson-Wagner, P. Tiffin, J. Wang, G. Zhang, J. Doebley, M. D. McMullen, D. Ware, E. S. Buckler, S. Yang, J. Ross-Ibarra, Comparative population genomics of maize domestication and improvement. *Nat. Genet.* **44**, 808–811 (2012).
55. J. Balarynová, B. Klčová, D. Tarkowská, V. Turečková, O. Trněný, M. Špundová, S. Ochatt, P. Smýkal, Domestication has altered the ABA and gibberellin profiles in developing pea seeds. *Planta* **258**, 25 (2023).
56. I. Ashikawa, F. Abe, S. Nakamura, Ectopic expression of wheat and barley *DOG1*-like genes promotes seed dormancy in Arabidopsis. *Plant Sci.* **179**, 536–542 (2010).
57. X. Yu, J. Han, L. Li, Q. Zhang, G. Yang, G. He, Wheat PP2C-a10 regulates seed germination and drought tolerance in transgenic Arabidopsis. *Plant Cell Rep.* **39**, 635–651 (2020).
58. G. Née, E. Obeng-Hinneh, P. Sarvari, K. Nakabayashi, W. J. J. Soppe, Secondary dormancy in *Brassica napus* is correlated with enhanced *BnaDOG1* transcript levels. *Seed Sci. Res.* **25**, 221–229 (2015).
59. Y. Feng, M. Liu, Z. Wang, X. Zhao, B. Han, Y. Xing, M. Wang, Y. Yang, A 4-bp deletion in the 5′UTR of *TaAFP-B* is associated with seed dormancy in common wheat (*Triticum aestivum* L.). *BMC Plant Biol.* **19**, 349 (2019).
60. N. Tang, S. Ma, W. Zong, N. Yang, Y. Lv, C. Yan, Z. Guo, J. Li, X. Li, Y. Xiang, H. Song, J. Xiao, X. Li, L. Xiong, MODD mediates deactivation and degradation of OsbZIP46 to negatively regulate ABA signaling and drought resistance in rice. *Plant Cell* **28**, 2161–2177 (2016).
61. N. Guo, S. Tang, Y. Wang, W. Chen, R. An, Z. Ren, S. Hu, S. Tang, X. Wei, G. Shao, G. Jiao, L. Xie, L. Wang, Y. Chen, F. Zhao, Z. Sheng, P. Hu, A mediator of OsbZIP46 deactivation and degradation negatively regulates seed dormancy in rice. *Nat. Commun.* **15**, 1134 (2024).
62. M. Koornneef, G. Reuling, C. M. Karssen, The isolation and characterization of abscisic acid-insensitive mutants of *Arabidopsis thaliana*. *Physiologia Plantarum* **61**, 377–383 (1984).
63. E. Nambara, M. Suzuki, S. Abrams, D. R. Mccarty, Y. Kamiya, P. Mccourt, A Screen for genes that function in abscisic acid signaling in *Arabidopsis thaliana*. *Genetics* **161**, 1247–1255 (2002).
64. S. L. Kendall, A. Hellwege, P. Marriot, C. Whalley, I. A. Graham, S. Penfield, Induction of dormancy in Arabidopsis summer annuals requires parallel regulation of *DOG1* and hormone metabolism by low temperature and CBF transcription factors. *Plant Cell* **23**, 2568–2580 (2011).
65. N. Xu, J. D. Bewley, The role of abscisic acid in germination, storage protein synthesis and desiccation tolerance in alfalfa (*Medicago sativa* L.) seeds, as shown by inhibition of its synthesis by fluridone during development. *J. Exp. Bot.* **46**, 687–694 (1995).
66. J. Takeuchi, M. Okamoto, R. Mega, Y. Kanno, T. Ohnishi, M. Seo, Y. Todoroki, Abscinazole-E3M, a practical inhibitor of abscisic acid 8′-hydroxylase for improving drought tolerance. *Sci. Rep.* **6**, 37060 (2016).
67. M. Romera-Branchat, E. Severing, C. Pocard, H. Ohr, C. Vincent, G. Née, R. Martinez-Gallegos, S. Jang, F. Andrés, P. Madrigal, G. Coupland, Functional divergence of the Arabidopsis florigen-interacting bZIP transcription factors FD and FDP. *Cell Rep* **31**, 107717 (2020).
68. K. W. Earley, J. R. Haag, O. Pontes, K. Opper, T. Juehne, K. Song, C. S. Pikaard, Gateway-compatible vectors for plant functional genomics and proteomics. *Plant J.* **45**, 616–629 (2006).
69. K. P. Lee, L. Lopez-Molina, A seed coat bedding assay to genetically explore in vitro how the endosperm controls seed germination in *Arabidopsis thaliana*. *J. Vis. Exp.* **2013**, e50732 (2013).
70. C. Koncz, J. Schell, The promoter of TL-DNA gene 5 controls MGG the tissue-specific expression of chimaeric genes carried by a novel type of *Agrobacterium* binary vector. *Mol. Gen. Genet.* **204**, 383–396 (1986).
71. F. Garabagi, E. Gilbert, A. Loos, M. D. McLean, J. C. Hall, Utility of the P19 suppressor of gene-silencing protein for production of therapeutic antibodies in Nicotiana expression hosts. *Plant Biotechnol. J.* **10**, 1118–1128 (2012).

72. S. Bensmihen, A. To, G. Lambert, T. Kroj, J. Giraudat, F. Parcy, Analysis of an activated ABI5 allele using a new selection method for transgenic Arabidopsis seeds. *FEBS Lett.* **561**, 127–131 (2004).
73. J. R. Wiśniewski, A. Zougman, N. Nagaraj, M. Mann, Universal sample preparation method for proteome analysis. *Nat. Methods* **6**, 359–362 (2009).
74. M. Hartl, A.-C. König, I. Finkemeier, Identification of lysine-acetylated mitochondrial proteins and their acetylation sites. *Methods Mol. Biol.* **1305**, 107–121 (2015).
75. Y. Xiang, B. Song, G. Née, K. Kramer, I. Finkemeier, W. J. J. Soppe, Sequence polymorphisms at the *REDUCED DORMANCY5* pseudophosphatase underlie natural variation in Arabidopsis dormancy. *Plant Physiol.* **171**, 2659–2670 (2016).
76. N. A. Kulak, G. Pichler, I. Paron, N. Nagaraj, M. Mann, Minimal, encapsulated proteomic-sample processing applied to copy-number estimation in eukaryotic cells. *Nat. Methods* **11**, 319–324 (2014).
77. J. Rappsilber, M. Mann, Y. Ishihama, Protocol for micro-purification, enrichment, pre-fractionation and storage of peptides for proteomics using StageTips. *Nat. Protoc.* **2**, 1896–1906 (2007).
78. P. Tilak, F. Kotnik, G. Née, J. Seidel, J. Sindlinger, P. Heinkow, J. Eirich, D. Schwarzer, I. Finkemeier, Proteome-wide lysine acetylation profiling to investigate the involvement of histone deacetylase HDA5 in the salt stress response of Arabidopsis leaves. *Plant J.* **115**, 275–292 (2023).
79. V. Krishnakumar, M. R. Hanlon, S. Contrino, E. S. Ferlanti, S. Karamycheva, M. Kim, B. D. Rosen, C.-Y. Cheng, W. Moreira, S. A. Mock, J. Stubbs, J. M. Sullivan, K. Krampis, J. R. Miller, G. Micklem, M. Vaughn, C. D. Town, Araport: The Arabidopsis information portal. *Nucleic Acids Res.* **43**, D1003–D1009 (2015).
80. J. Cox, M. Y. Hein, C. A. Luber, I. Paron, N. Nagaraj, M. Mann, Accurate proteome-wide label-free quantification by delayed normalization and maximal peptide ratio extraction, termed MaxLFQ. *Mol. Cell. Proteomics* **13**, 2513–2526 (2014).
81. S. Tyanova, T. Temu, P. Sinitcyn, A. Carlson, M. Y. Hein, T. Geiger, M. Mann, J. Cox, The Perseus computational platform for comprehensive analysis of (prote)omics data. *Nat. Methods* **13**, 731–740 (2016).
82. M. E. Ritchie, B. Phipson, D. Wu, Y. Hu, C. W. Law, W. Shi, G. K. Smyth, limma powers differential expression analyses for RNA-sequencing and microarray studies. *Nucleic Acids Res.* **43**, e47 (2015).
83. S. Maere, K. Heymans, M. Kuiper, BiNGO: A Cytoscape plugin to assess overrepresentation of Gene Ontology categories in Biological Networks. *Bioinformatics* **21**, 3448–3449 (2005).
84. P. Shannon, A. Markiel, O. Ozier, N. S. Baliga, J. T. Wang, D. Ramage, N. Amin, B. Schwikowski, T. Ideker, Cytoscape: A software environment for integrated models of biomolecular interaction networks. *Genome Res.* **13**, 2498–2504 (2003).
85. J. Mergner, M. Frejno, M. List, M. Papacek, X. Chen, A. Chaudhary, P. Samaras, S. Richter, H. Shikata, M. Messerer, D. Lang, S. Altmann, P. Cyprys, D. P. Zolg, T. Mathieson, M. Bantscheff, R. R. Hazarika, T. Schmidt, C. Dawid, A. Dunkel, T. Hofmann, S. Sprunck, P. Falter-Braun, F. Johannes, K. F. X. Mayer, G. Jürgens, M. Wilhelm, J. Baumbach, E. Grill, K. Schneitz, C. Schwechheimer, B. Kuster, Mass-spectrometry-based draft of the Arabidopsis proteome. *Nature* **579**, 409–414 (2020).
86. L. D. Vu, T. Zhu, I. Verstraeten, B. van de Cotte, International Wheat Genome Sequencing Consortium, K. Gevaert, I. De Smet, Temperature-induced changes in the wheat phosphoproteome reveal temperature-regulated interconversion of phosphoforms. *J. Exp. Bot.* **69**, 4609–4624 (2018).
87. J. Qiu, Y. Hou, X. Tong, Y. Wang, H. Lin, Q. Liu, W. Zhang, Z. Li, B. R. Nallamilli, J. Zhang, Quantitative phosphoproteomic analysis of early seed development in rice (*Oryza sativa* L.). *Plant Mol. Biol.* **90**, 249–265 (2016).
88. A. Rodrigues, M. Adamo, P. Crozet, L. Margalha, A. Confraria, C. Martinho, A. Elias, A. Rabissi, V. Lumbreras, M. González-Guzmán, R. Antoni, P. L. Rodriguez, E. Baena-González, ABI1 and PP2CA phosphatases are negative regulators of Snf1-related protein kinase1 signaling in Arabidopsis. *Plant Cell* **25**, 3871–3884 (2013).
89. F. Vlad, S. Rubio, A. Rodrigues, C. Sirichandra, C. Belin, N. Robert, J. Leung, P. L. Rodriguez, C. Laurière, S. Merlot, Protein phosphatases 2C regulate the activation of the Snf1-related kinase OST1 by abscisic acid in Arabidopsis. *Plant Cell* **21**, 3170–3184 (2009).


**Acknowledgments:** We thank R. Finkelstein (University of California, Santa Barbara) for providing the *35S::YFP:AFP2* (+/−) transgenic and *abi5-7* mutant lines and L. Lopez-Molina (University of Geneva) for providing the AFP1 antibody. We thank G. Brun and S. Weinl (University of Muenster) for providing an aliquot of ABZ-E3M and support for isotope related work, respectively. We also thank A. Harzen (MPI Cologne) for MS sample preparation and E. Felgenhauer and T. Willenborg (University of Muenster) for technical support during seed batch production/processing and mutant genotyping. We thank P. Heinkow (University of Münster) for technical assistance and for maintaining the LC-MS/MS instruments at the MSPUB. We dedicate this work to our friend and former colleague F.A. who passed away on 4 August 2019 at the age of 28. **Funding:** This work was supported by the Deutsche Forschungsgemeinschaft grant no. NE2296 to G.N. and grant number 469950637 to I.F. as well as INST 211/744-1 FUGG for instrumentation. In addition, this work was supported by funding from the Max-Planck Society (I.F., K.K., G.N., and W.J.J.S.). T.K. was supported by a fellowship of the Studienstiftung des deutschen Volkes and by the department of biology of the University of Muenster. The research stay of F.A. at the University of Muenster was funded by the DAAD. Open access funding was provided by the University of Muenster.
**Author contributions:** G.N. conceived the study, applied for funding, and designed the experiments. T.K. and G.N. performed most of the experiments with the help of D.B. for Y2H assay, C.B. for co-IP assays, J.S., E.G., F.A., M.G., J.D., and D.B. during mutant isolation and phenotyping. D.B., J.S., M.G., J.D., E.G., and C.B. conducted their experiments as integral components of their degree programs at the University of Muenster. M.R.-B. performed transcript analysis. I.F., J.E., and K.K. provided MS measurements and support for method development, Max Quant and Perseus analyses. I.F. provided funding support and supervision. G.N. supervised the project, analyzed the data with the help of T.K., and drafted the manuscript. G.N. wrote the final version, with edits from T.K., W.J.J.S., and I.F. **Competing interests:** The authors declare that they have no competing interests. **Data and materials availability:** Mass spectrometry proteomic data have been deposited in the ProteomeXchange Consortium (http://proteomecentral.proteomexchange.org) via the JPOSTDB partner repository with the data set identifiers PXD046985 and PXD053457. Sequence data from this article can be found in The Arabidopsis Information Resource-TAIR database (www.arabidopsis.org) under the following accession numbers: AFP1 (AT1G69260), AFP2 (AT1G13740), AFP3 (AT3G29575), AFP4 (AT3G02140), AHG1 (AT5G51760), AHG3 (AT3G11410), ABI1 (AT4G26080), ABI2 (AT5G57050), HAB1 (AT1G72770), HAB2 (AT1G17550), HAI1 (AT5G59220), HAI2 (AT1G07430), HAI3 (AT2G29380), SnRK2.6 (AT4G33950), SnRK1a1 (AT3G01090); or the UniProt database (https://uniprot.org/) under the following accession numbers: OsMODD (Q10Q07), TaAFP-B (B1B5D4), OsPP2C37 (Q7XP01) and TaPP2C-a10 (A0A3B6ANL1). All other data needed to evaluate the conclusions in the paper are present in the paper and/or the Supplementary Materials.

Submitted 18 July 2024
Accepted 28 January 2025
Published 28 February 2025
10.1126/sciadv.adr8502